KeAi

CHINESE ROOTS
GLOBAL IMPACT

Contents lists available at ScienceDirect

Petroleum Science

journal homepage: www.keaipublishing.com/en/journals/petroleum-science



Original Paper

High-temperature and high-salinity resistance hydrophobic association zwitterionic filtrate loss reducer for water-based drilling fluids



Tai-Feng Zhang a,b , Jin-Sheng Sun a,b,* , Jing-Ping Liu a,b,** , Kai-He Lv a,b , Yuan-Wei Sun a,b , Zhe Xu a,b , Ning Huang a,b , Han Yan a,b

ARTICLE INFO

Article history: Received 19 December 2024 Received in revised form 20 May 2025 Accepted 20 May 2025 Available online 20 May 2025

Edited by Jia-Jia Fei

Keywords:
High-temperature
High-salinity
Hydrophobic association
Zwitterionic
Filtrate loss reducer
Water-based drilling fluids

ABSTRACT

As the global exploration and development of oil and gas resources advances into deep formations, the harsh conditions of high temperature and high salinity present significant challenges for drilling fluids. In order to address the technical difficulties associated with the failure of filtrate loss reducers under high-temperature and high-salinity conditions. In this study, a hydrophobic zwitterionic filtrate loss reducer (PDA) was synthesized based on N,N-dimethylacrylamide (DMAA), 2-acrylamido-2-methylpropane sulfonic acid (AMPS), diallyl dimethyl ammonium chloride (DMDAAC), styrene (ST) and a specialty vinyl monomer (A₁). When the concentration of PDA was 3%, the FL_{API} of PDA-WBDF was 9.8 mL and the FL_{HTHP} (180 °C, 3.5 MPa) was 37.8 mL after aging at 240 °C for 16 h. In the saturated NaCl environment, the FL_{API} of PDA-SWBDF was 4.0 mL and the FL_{HTHP} (180 °C, 3.5 MPa) was 32.0 mL after aging at 220 °C for 16 h. Under high-temperature and high-salinity conditions, the combined effect of anti-polyelectrolyte and hydrophobic association allowed PDA to adsorb on the bentonite surface tightly. The sulfonic acid groups of PDA increased the negative electronegativity and the hydration film thickness on bentonite surface, which enhanced the colloidal stability, maintained the flattened lamellar structure of bentonite and formed an appropriate particle size distribution, resulting in the formation of dense mud cakes and reducing the filtration loss effectively.

© 2025 The Authors. Publishing services by Elsevier B.V. on behalf of KeAi Communications Co. Ltd. This is an open access article under the CC BY-NC-ND license (http://creativecommons.org/licenses/by-nc-nd/4.0/).

1. Introduction

There is substantial oil and gas resources with great potential for exploration and development all over the world (Mu and Ji, 2019). Safe and efficient development of deep oil and gas resources is of paramount importance for ensuring national energy security and accelerating the transition towards carbon peak and carbon neutrality. Drilling is the core engineering of deep oil and gas exploration and development. As the depth of drilling increases, the geological conditions of deep formations become

Peer review under the responsibility of China University of Petroleum (Beijing).

more complex. The technical challenge of deep oil and gas resources development is to ensure safe, efficient and low-cost drilling (Yao et al., 2018; Sun et al., 2024).

As the "blood" of drilling engineering, drilling fluids play the essential roles in balancing formation pressure, maintaining wellbore stability, suspending and carrying bit cuts, cleaning well bottom, etc., which is one of the key technologies to ensure drilling safety of deep wells (Gautam and Guria, 2020; Jiang et al., 2020). Water-based drilling fluids (WBDFs) are a kind of colloidal dispersion system composed of bentonite, water and additives. They are widely used in oil fields with advantages of low cost, environment friendly and convenient recycling (Li et al., 2024; Huang et al., 2023). However, filtrate loss reducers are susceptible to invalidate under high-temperature (220 °C) and high-salinity (≥15% NaCl) conditions, which leads to deterioration of rheology and filtration loss of drilling fluids. There will be prone to cause wellbore collapse, stuck drilling, blowout and other

^a State Key Laboratory of Deep Oil and Gas, China University of Petroleum (East China), Qingdao, 266580, Shandong, China

^b School of Petroleum Engineering, China University of Petroleum (East China), Qingdao, 266580, Shandong, China

^{*} Corresponding author.

^{**} Corresponding author.

E-mail addresses: sunjsdri@cnpc.com.cn (J.-S. Sun), Liujingping20@126.com (J.-P. Liu).

downhole complex problems, even evolving into a "well destruction" catastrophic accidents (Katende et al., 2019; Lu et al., 2024) that severely impede the efficiency and safety of deep wells drilling engineering.

The filtrate loss reducers could be classified into natural modified polymers and synthetic polymers. Natural modified polymers (e.g. sodium humate, carboxy methyl starch, sodium carboxymethyl cellulose, etc.) exhibited limited resistance to hightemperature and high-salinity, they were unable to meet the requirements of drilling operations. Synthetic polymers were highly designable due to adjustable molecular weight, composition, and the number of functional groups (Sepehri et al., 2018). Researchers used different kinds of vinyl monomers to prepare a variety of filtrate loss reducers (Abdollahi et al., 2018; Li et al., 2023a; Davoodi et al., 2023a). Especially following the large-scale promotion of 2-acrylamide-2-methylpropanesulfonic acid (AMPS), the filtrate loss reducers most frequently reported were anionic polymers based on acrylamide (AM) and AMPS. Dickert and Heilweil (1986) reported a kind of vinylsulfonate-vinylamide copolymer prepared by AM, AMPS and N-vinyl-N-methylacetamide. The molecular weight of the polymer was from 10⁶ to 2×10^6 . The temperature resistance of the copolymer was up to 200 °C, but it was only resistant to 0.8% NaCl. Tehrani synthesized a terpolymer by using AM, AMPS and N-vinylpyrrolidone (NVP) (Tehrani et al., 2009). The polymer exhibited temperature resistance up to 232 °C in freshwater drilling fluids. Wu et al. (2001) used AM, AMPS, NVP and itaconic acid (IA) to prepare a quaternary copolymer by free radical polymerization. The filtration loss of drilling fluids could be controlled under 220 °C and 4% NaCl conditions effectively with the copolymer. Anionic polymers were purely negatively charged. Their molecular chains were fully extended in freshwater. However, as the concentration of metal cations (such as Na⁺, K⁺, Ca²⁺) increased, the negative charge of the anionic groups was shielded by metal cations, resulting in molecular chains curling, leading to the deterioration of adsorption and hydration capacity of polymers (Muthukumar, 2017).

The zwitterionic polymers were polyelectrolytes containing both anions and cations in their molecular chains. With the concentration of metal cations growth, the electrostatic attraction between the anions and cations of zwitterionic polymers was shielded by metal cations. The "inernal salt bonds" was disrupted and the cationic groups and anionic groups were released. In contrast to anionic polymers, it was conducive to strengthen the adsorption capacity and hydration capacity of polymers to maintain the colloidal stability of bentonite and reducing the filtration loss even under the negative influence of high concentrations of NaCl (Blackman et al., 2019; Jhan and Tsay, 2014; Kumar and Fredrickson, 2009; Oriji and Dosunmu, 2012). Lucas et al. (1981) prepared a zwitterionic polymer by free radical polymerization of vinyl amide, vinyl sulphonate and diallyl dimethyl ammonium chloride, which was found to improve the rheology of drilling fluids and reduce the filtration loss under 204 °C and saturated salt conditions (Son et al., 1987). Li et al. (2022) prepared a microcrosslinked zwitterionic gel DDAM by using DMAA, AMPS, MA, and DMDAAC as monomers and the triallylamine as the crosslinker. With 2% DDAM, the FL_{API} was 8.0 mL under 200 °C and saturated salt conditions. Ma et al. (2020) synthesized a zwitterionic copolymer PADAN by combining a betaine monomer DMAPMAS with AM, AMPS, and NVP. Under 200 °C and saturated salt conditions, the FL_{API} was reduced to 4.0 mL with 2.0% PADAN. Zhao et al. (2015) synthesized a zwitterionic copolymer by using N, N-dimethylacrylamide (DMAA), AMPS, DMDAAC, and NVP. The FLAPI could be controlled at 20.6 mL with 2% copolymer under 220 °C and saturated NaCl conditions. Furthermore, incorporation of hydrophobic monomers and rigid groups had been revealed to enhance the temperature and salt resistance of polymers. Sun et al. (2022a) synthesized a hydrophobic association copolymer ASML through emulsion polymerization with AM, sodium styrene sulfonate (SSS), maleic anhydride (MA) and lauryl methacrylate (LMA) as the materials, odium dodecyl sulphate (SDS) as the emulsifier. When the concentration of ASML was 3%, the FL_{APl} of drilling fluids was only 5.0 mL under 200 °C and 30% NaCl conditions. Li et al. (2023b, 2023c, 2023d) prepared a filtration loss reducer DAAS by using DMAA, AMPS with rigid cyclic monomers 4-acryloylmorpholine (ACMO) and SSS. It was able to control the FL_{APl} of drilling fluids to 7.6 mL under 200 °C and saturated salt conditions.

There was a wide range of filtrate loss reducers available recently, but their temperature resistance was only up to 200 °C under saturated salt condition. They were incompetent for use in the ultra-high-temperature (220 °C) environment (Davoodi et al., 2023b; Gautam et al., 2022). In this study, a hydrophobic association zwitterionic filtrate loss reducer (PDA) was synthesized based on DMAA, AMPS, DMDAAC, ST and a specialty vinyl monomer (A_1) through emulsion polymerization. The high-temperature hydrolysis-resistant amide groups, rigid quaternary ammonium five-membered rings, benzene rings and sulfonic acid groups endowed PDA with excellent high-temperature resistance. The highly hydratable sulfonic acid groups of AMPS were able to enhance the salt tolerance of PDA. The cationic monomer DMDAAC was chosen to strengthen the adsorption capacity of PDA on the bentonite surface. Under high-temperature and high-salinity conditions. PDA was capable of forming a robust physical crosslinking network through hydrophobic association, reinforcing the temperature resistance of the polymer. It also limited the internal rotation and preventing the thermal movement of the molecular chain, which made PDA less susceptible to desorb from bentonite surface. The effect of anti-polyelectrolyte facilitated the extension of the polymer. Increased rotation radius and hydrodynamic volume made PDA adsorb on the bentonite tightly, increasing the hydration film thickness of bentonite surface, protecting the colloidal stability of bentonite (Sun et al., 2020; Tonge and Tighe, 2001). Consequently, PDA was able to control the filtration loss of drilling fluids under 220 °C and saturated salt conditions, supporting the safety and efficiency of drilling deep and ultra deep wells.

2. Experimental section

2.1. Materials

2-acrylamido-2-methylpropanesulfonic acid (AMPS, 98%), dimethyl diallyl ammonium chloride (60% aqueous solution), styrene (ST, 99.5%), N,N-dimethylacrylamide(DMAA, 98%) were purchased from McLean Biochemicals (Shanghai, China), sodium hydroxide (NaOH, 95%), sodium dodecyl sulphate (SDS, 99%), sodium chloride (NaCl, 99.5%), anhydrous sodium carbonate (Na₂CO₃, 99.5%), 2,2'-azobis (2-methylpropionamidine) dihydrochloride (V50, 97%) were provided by Shanghai Aladdin Biochemical Technology Co. Bentonite was purchased from Huai'an Tengfei County Bentonite Co. Ltd. SP-1 and SP-2 are sulfonate polymers currently used on a large scale in oil fields of China, which were offered by Shandong Deshunyuan Petroleum Technology Co. Ltd. The specialty vinyl monomer (A_1) was bought from Beijing Konojie energy environmental protection Technology Co. Ltd. Driscal D and Dristemp were purchaed from Drilling Specialties Company.

2.2. Synthesis of copolymer PDA

The hydrophobic association zwitterionic filtrate loss reducer (PDA) was prepared through emulsion polymerization, the molar ratio (DMAA:AMPS:DMDAAC:A₁:ST) was 6:3:1:1:0.5, the mass fraction of monomers was 35 wt%. As shown in Fig. 1, a certain mass of AMPS (10.15 g. 0.049 mol) was dissolved in deionized water firstly, the pH of the solution was adjusted to 7.0 with 10 mol/L NaOH solution. Subsequently, DMAA (14.57 g, 0.147 mol), DMDAAC (3.96 g, 0.0245 mol), A₁ (6.89 g, 0.0245 mol) were added into the solution. The system was stirred at the rate of 1000 rpm for 5 min to make the monomers disperse evenly. Then, 0.03 g SDS and ST (1.28 g, 0.123 mol) were added. The system continued stirring for 20 min at 1000 rpm to form a stable emulsion (Zhang et al., 2019). And then, the system was transferred to a threenecked flask. After the system reached 65 °C, a certain mass of V50 was added to initiate polymerization. Finally, a viscous and off-white product was obtained by reacting for 4 h under nitrogen atmosphere. The product was precipitated in mixed solution of anhydrous ethanol and acetone, and filtered, dried to constant weight in a vacuum oven at 105 °C, crushed into powder to obtain the hydrophobic association zwitterionic copolymer PDA.

2.3. Characterization and analysis of PDA

The specialty vinyl monomer (A_1) and PDA were characterized by the IRTRacer-100 Fourier infrared spectrometer (Shimadzu, Japan) with the resolution of 0.25 cm $^{-1}$ and the scanning range of $460-4000 \ \text{cm}^{-1}$.

The specialty vinyl monomer (A₁) and PDA were separately dissolved in D₂O, the nuclear magnetic resonance hydrogen spectrum (¹H NMR) were performed by the Bruker AV III NMR spectrometer (Bruker Corporation, Germany).

The elemental composition of PDA was analyzed by the Elementar Unicube elemental analyzer (Elementar, Germany). The thermal stability of PDA in N_2 atmosphere was determined by TGA-2 thermogravimetric analyzer (METTLER TOLEDO, America) from 30 to 600 °C, the heating rate was 10 °C/min.

The molecular weight of PDA was determined by the 1260 Infinity II GPC/SEC gel permeation chromatograph (Agilent, America). Firstly, 20 mg of PDA was added in 10 mL water (deionized water with 0.1 M NaNO3) and kept static at 25 $^{\circ}\text{C}$ for 24 h, stirring for several times during the period to promote PDA dissolution. And then, the solution was filtered with microfiltration membranes (0.22 μm) to remove insoluble polymer. Finally, the clarified solution was fed into the gel chromatography column for measurement.

2.4. Characterisation of PDA in salt solutions

The PDA-salt solutions were prepared by adding 3% (w/v) PDA and different amount of NaCl (w/v) into deionized water and stirring at 5000 rpm for 20 min. The transmittance of PDA-salt solutions was tested by the UV-3600Plus UV spectrophotometer (Shimadzu, Japan), the range of wavenumber was from 200 to 800 cm⁻¹. The micro-morphology of PDA in salt solutions was observed by the JEM-2100 UHR transmission electron microscope (Nippon Electron, Japan).

2.5. Preparation of drilling fluids

Bentonite (40 g) and Na_2CO_3 (1.40 g) were added into water, the system was stirred for 2 h at the speed of 2000 rpm, then keeping static for 24 h to prepare water-based drilling fluids (WBDFs). A certain amount (w/v) of NaCl was added into 400 mL WBDFs and the system was kept stirring at the speed of 3000 rpm for 20 min to

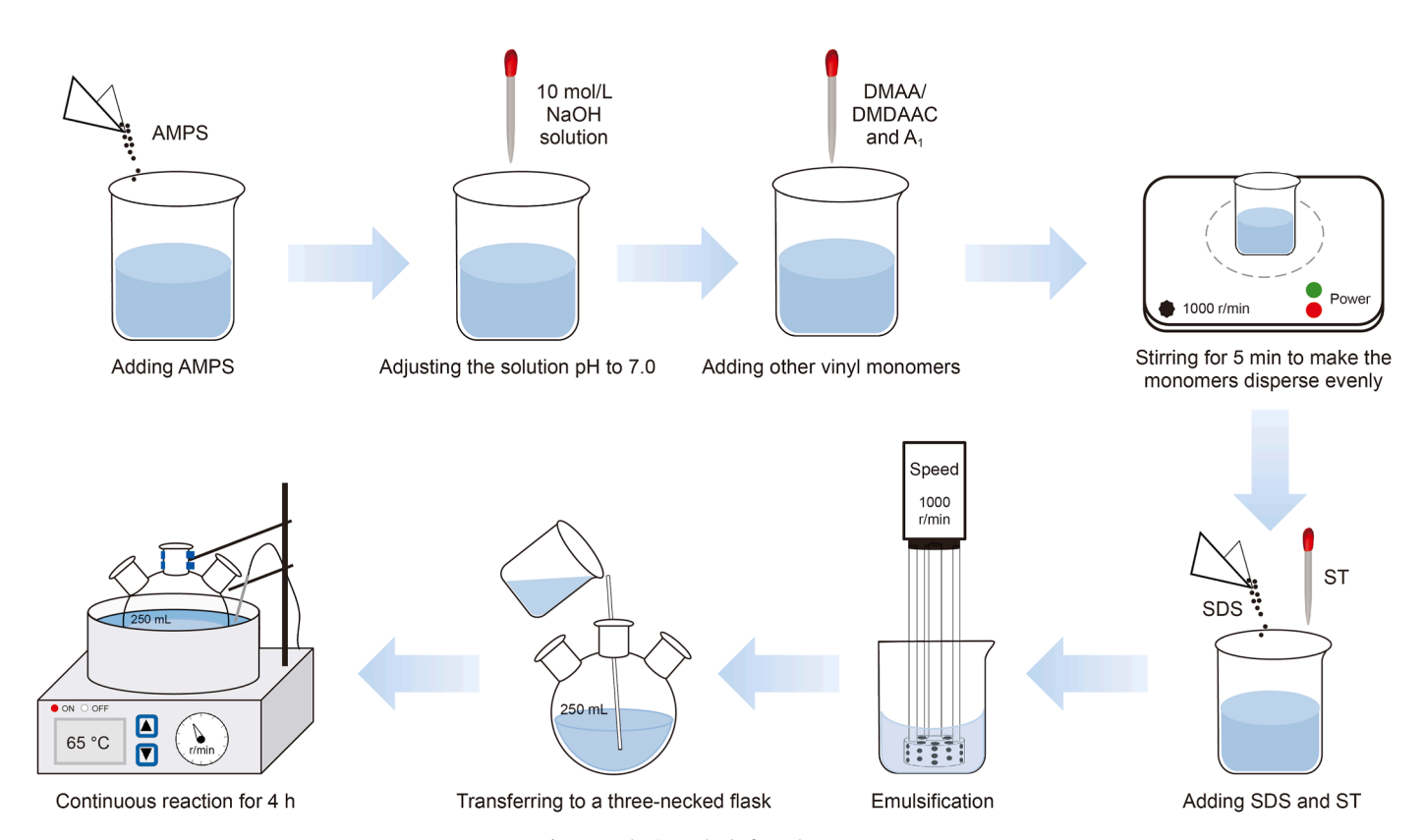


Fig. 1. Synthesis method of copolymer PDA.

obtain salt water-based drilling fluids (SWBDFs). PDA-water based drilling fluids (PDA-WBDFs) were prepared by adding a certain amount (w/v) of PDA into 400 mL WBDFs and keeping stirring at the speed of 8000 rpm for 20 min. The PDA-salt water-based drilling fluids (PDA-SWBDFs) were prepared by adding a certain amount of NaCl (w/v) into 400 mL PDA-water based drilling fluids and keeping stirring at the speed of 5000 rpm for 20 min.

2.6. Performance evaluation of drilling fluids

Based on the American Petroleum Institute (API) standard, the six-speed rotor viscometer ZNN-D6 (Qingdao Tongchun Petroleum Instrument Co., Ltd., China) was used to measure the readings of each drilling fluid at 600 and 300 rpm, recorded as θ_{600} , θ_{300} respectively. The apparent viscosity (AV, mPa·s), plastic viscosity (PV, mPa·s), and yield point (YP, Pa) were calculated according to the following equation:

$$AV = 0.5 \times \theta_{600} \; (mPa \cdot s)$$

$$PV = \theta_{600} - \theta_{300} \; (mPa {\cdot} s)$$

$$YP = 0.511 \times (\theta_{300} - PV) (Pa)$$

The SD6A medium pressure filtration loss instrument (Qingdao Tongchun Petroleum Instrument Co., China) was used to measure the API filtration loss (FL_{API}) of drilling fluids at the conditions of 0.69 \pm 0.03 MPa and 25 °C. The GGS71-B high-temperature high-pressure filtration loss instrument (Qingdao Tongchun Petroleum Instrument Co., China) was used to measure the HTHP filtration loss (FL_{HTHP}). High-temperature high-pressure aging tests were carried out in a rolling heating furnace for 16 h at the experiment temperatures.

2.7. Mechanism of filtration loss reduction via PDA

The adsorption capacity of PDA was determined by TOC-L total organic carbon analyzer (Shimadzu, Japan). Each sample was measured five times, the final result was the average of the five measurements. The adsorption capacity (AC) of PDA was calculated by the following equation (Sun et al., 2022b):

$$AC = \frac{m_1 - m_2 \times \frac{m_c}{C}}{m_0}$$

AC represents the adsorption amount of PDA on the bentonite surface (mg/g); m_1 is the initial mass of PDA in the drilling fluids (g); m_2 is the filtrate mass of the high-temperature and high-pressure filtration loss test (g); m_0 is the initial mass of the bentonite in the drilling fluid (g); m_0 is the TOC of the filtrate (mg/L); C is the mass fraction of carbon in PDA, which is determined by elemental analysis.

The PDA-SWBDFs were added dropwise to the specimen stage, put into liquid nitrogen slush for quick-freezing for 30 s, sublimated at $-90\,^{\circ}\text{C}$ for 10 min. And then they were sprayed with gold and sent to the scanning electron microscope room for observation. The temperature of cold stage was $-140\,^{\circ}\text{C}$, the accelerating voltage was 5 kV.

The drilling fluids were diluted 1000 times in deionized water. The zeta potential of drilling fluids was tested by the Nano ZS90 Zeta Potential Analyzer (Malvern, UK). Each sample was carried out for three times, the final result was the average of three measurements.

The particle size distribution of drilling fluids before and after aging at 220 °C were measured through Mastersizer-3000E

(Malvern, UK). In the experiment, the concentration of NaCl was 36% in SWBDFs and PDA-SWBDFs.

The mud cakes of drilling fluids after API filtration loss test and HTHP filtration loss test were vacuum dried at 60 °C to constant weight, the micro-morphology of mud cakes was observed by the EVO-15/LS scanning electron microscope (Zeiss, Germany).

The dried powder of mud cakes was ultrasonically dispersed in deionized water for 10 min and then placed on the copper grid. After water evaporated, the microstructure of the bentonite was observed by the JEM-2100 UHR (Nippon Electron) transmission electron microscope.

3. Results and discussion

3.1. Characterization and analysis of PDA

3.1.1. Molecular structure characterisation of PDA

The infrared spectrogram of the specialty monomer A₁ is shown in Fig. 2(a), the characteristic peak located at 2935 cm⁻¹ was the asymmetric stretching vibration of C–H in the methylene group, the characteristic peaks located at 1546 and 1400 cm⁻¹ came from the backbone vibration of the benzene rings. The characteristic peaks located at 1460 cm⁻¹ should be from quaternary ammonium cations (Huang et al., 2024). The characteristic peaks located at 1219, 1186, and 1037 cm⁻¹ could be linked with the stretching vibrations of S=O and S-O bonds of sulfonic acid groups (Liu et al., 2024). The characteristic peaks located at 995 and 905 cm⁻¹ belong to the out-of-plane deformation vibration of -CH=CH₂, the characteristic peak at 626 cm⁻¹ was from the stretching vibration of the C–S bond. These peaks corresponded to the functional groups of benzene ring, quaternary ammonium cation and sulfonic acid group in the specialty monomer A₁.

The $^1\text{H-NMR}$ of the specialty monomer A_1 is shown in Fig. 2(b), the characteristic peak located at 1.619 ppm was from the chemical shift of H in $-\text{CH}_2-\text{SO}_3$. The characteristic peak located at 2.632 ppm represented the chemical shift of H in CH_2 connected with the benzene ring. The characteristic peaks located at 2.932 and 3.095 ppm could be related with H in $-\text{CH}_2-\text{N}^+$ and CH_3-N^+ (Luo et al., 2023; Zhong et al., 2023). The characteristic peaks located at 5.252, 5.701 and 6.720 ppm came from the chemical shift of H on the C=C double bond connected with the benzene ring. The characteristic peaks located at 7.465 and 7.668 ppm belong to the chemical shift of H in the benzene ring (Liu et al., 2022a). The $^1\text{H-NMR}$ of A_1 was corresponding with its infrared spectrogram.

The infrared spectrogram of PDA is shown in Fig. 2(c), the characteristic peak located at 3502 cm⁻¹ came from the stretching vibration of the N-H bond in the amide group. The characteristic peaks at 1728 and 1629 cm⁻¹ should be linked with the C=O telescopic stretching vibrations in AMPS. The characteristic peak located at 2935 cm⁻¹ could be attributed to the asymmetric stretching vibration of the C-H bond in -CH2. The vibrational absorption peak of the C-N bond in the five-membered ring of the quaternary ammonium cation should be at 1460 cm⁻¹. The characteristic peaks at 1546 and 1400 cm⁻¹ should belong to the backbone vibrations of the benzene rings. The characteristic peaks at 1219, 1186 and 1037 cm⁻¹ derived from the stretching vibrations of S-O and S=O in the sulfonic acid moiety. The characteristic peak at 626 cm⁻¹ represented the stretching vibration of the C-S bond. The infrared spectroscopy of PDA contained all of characteristic peaks of the specialty monomer A_1 .

The $^1\text{H-NMR}$ of PDA is shown in Fig. 2(d), the peak at 1.455 ppm represented the chemical shift of -CONH- in AMPS, the chemical shift of $C-(\text{CH}_3)_2$ —in AMPS was at the peak of 1.503 ppm (Gao et al., 2024), the peak at 1.619 ppm could be related with the chemical shift of $-\text{CH}_2-\text{SO}_3$ in AMPS. The peak at 2.720 ppm was relevant to

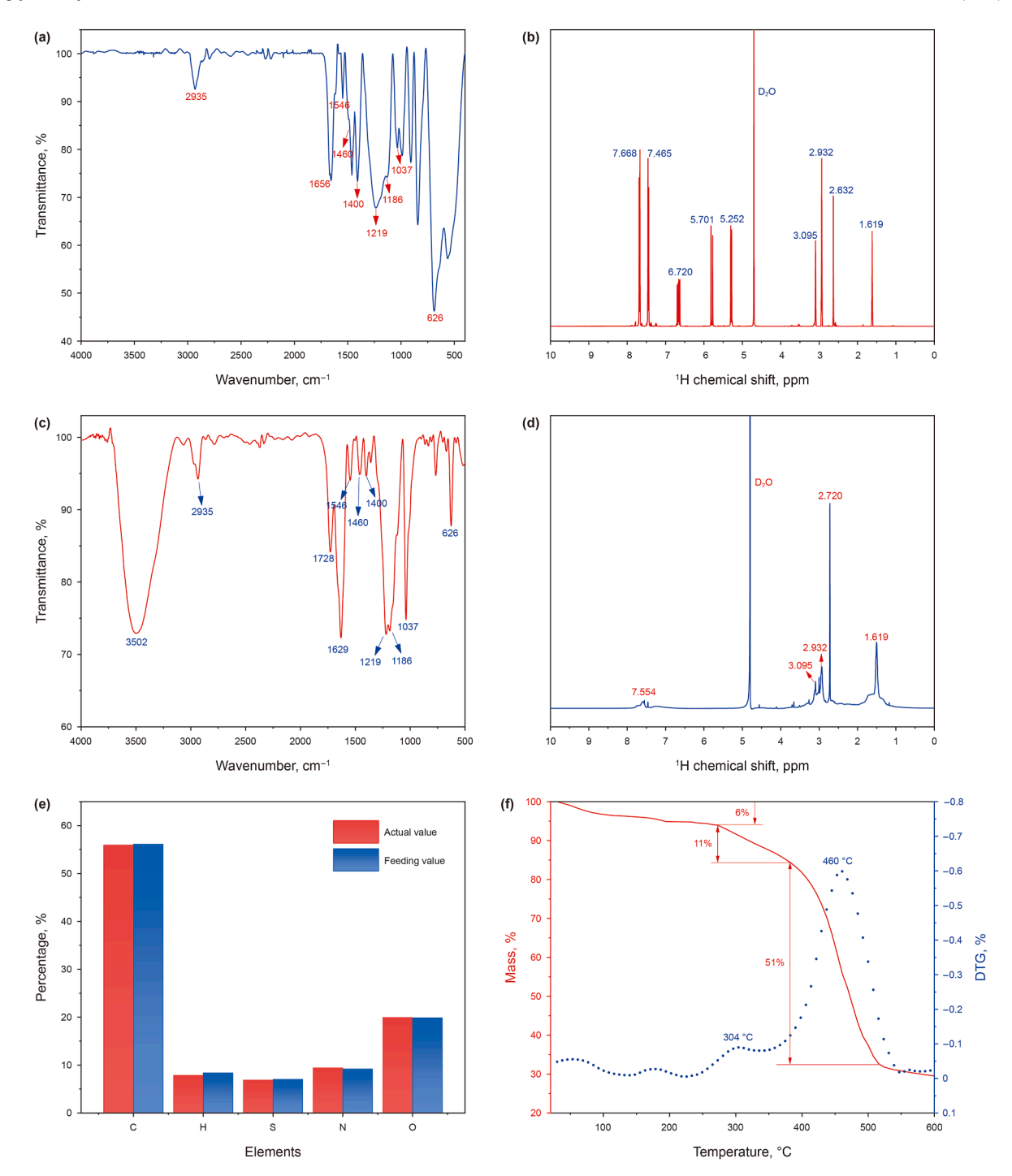


Fig. 2. Molecular structure characterisation of specialty vinyl monomer A₁ and copolymer PDA: (**a**) infrared spectrogram of A₁; (**b**) ¹H NMR analysis of A₁; (**c**) infrared spectrogram of PDA; (**d**) ¹H NMR analysis of PDA; (**e**) elemental analysis of PDA; (**f**) TGA and DTG analysis of PDA.

the chemical shift of $-CH_2-CH-CO-$, $-CH_2-CH-$. The chemical shift of CH_3-N^+ and CH_2-N^+ in DMDAAC were at the peak of 2.932, 3.095 ppm respectively. The overlapping multiple peaks at 7.554 ppm indicated the chemical shift of the H in the benzene ring. The 1H NMR analysis of PDA showed that PDA contained all functional groups of raw materials, which validated the successful polymerization of PDA.

The results of elemental analysis are shown in Fig. 2(e), which showed that the proportion of C, H, S, N, O in the product was 56.73%, 9.36%, 5.96%, 9.85%, 18.10% respectively. With the calculation of above data, the actual molar ratio of five unit structures (DMAA:AMPS:

DMDAAC:A₁:ST) was 6.053:1.896:0.912:0.887:0.432 in the product. According to the dosing molar ratio (DMAA:AMPS:DMDAAC: A₁:ST = 6:2:1:1:0.5), the theoretical proportion of C, H, S, N, O in the product was 56.12%, 9.36%, 7.01%, 9.20%, 19.86%. The results of elemental analysis revealed that the actual molar ratio was nearly corresponding with the dosing molar ratio. The results of FTIR, 1 HNMR and elemental analysis illustrated that the product was the target copolymer.

At the bottom of deep wells, the temperature can reach 220 °C, even 240 °C. The thermal stability of filtrate loss reducers will determine whether they can be applied in ultra-high-temperature

Table 1GPC analysis of PDA.

Molecular weight	$M_{\rm n}$	M_{w}	$M_{ m p}$
Dalton	425562	865046	835287

environment. The thermogravimetric curve of PDA is shown in Fig. 2(f), there were four stages of mass loss of PDA during temperature ranging from 30 to 600 °C. The first stage was 30–265 °C, the curve was flat which showed that the thermal degradation rate was slow (Tang et al., 2022). The mass loss of PDA was 5% which was mainly from the evaporation of intermolecular free water and bound water adsorbed on amide and sulfonic acid groups. The second stage was 265-380 °C, the thermal degradation of amide groups resulted in the 11% decrease of total mass of PDA. The third stage was 380-510 °C, due to the thermal degradation of a large number of amide groups, sulfonic acid groups, benzene rings, the mass loss of PDA was 51% with the maximum rate of degradation at 460 $^{\circ}$ C in this stage. The fourth stage was 510–600 $^{\circ}$ C, where the C–C bond in the main chain of PDA was broken. There was only 17% mass loss of PDA at 380 °C, which revealed that PDA had excellent thermal stability. PDA is suitable for temperature resistant filtrate reducer for drilling fluids in deep wells.

The results of GPC are shown in Table 1. The weight-average molecular weight $(M_{\rm w})$ of PDA was 865046. The number-average molecular weight $(M_{\rm n})$ of PDA was 425562. PDA had a moderate molecular weight. The PDI was 2.032, indicating that the distribution of molecular weight of PDA was narrow, which showed there was a good effect of polymerization of PDA (Liu et al., 2020).

3.1.2. Characterisation of PDA in salt solutions

The hydrophobic association effect of PDA was verified macroscopically by observing the appearance of the polymer solutions and measuring the transmittance of the PDA salt solutions. The appearance of PDA salt solutions with different amounts of NaCl is shown in Fig. 3(a). The PDA salt solutions with 0% NaCl and 5% NaCl appeared more transparent, whereas the solutions with 15% NaCl, 25% NaCl and 36% NaCl were more turbid obviously. The UV spectral analysis of PDA salt solutions is shown in Fig. 3(b), where the transmittance of the solutions decreased gradually with

the increase of NaCl concentration. This phenomenon could be attributed to the hydrophobic association of the polymer, which resulted in the formation of water-insoluble hydrophobic microregions (Chang et al., 2019). The process led to the turbidity of the solutions and the decrease of the transmittance.

The micromorphology of the hydrophobic association of PDA was successfully observed by TEM, as illustrated in Fig. 3(c). When the concentration of NaCl was 0%. PDA exhibited the curled-up or linear shape, because there was electrostatic attraction between the quaternary ammonium cations and the sulfonic acid groups. When the concentration of NaCl was 15%, a large number of hydrophobic micro-regions could be observed from the figure (black cluster-like regions). It might have been caused by the stretch of the molecular chains of PDA, enabling the formation of a threedimensional network through hydrophobic association. When the concentration of NaCl increased to 25%, the size of hydrophobic micro-regions became larger. The three-dimensional network could still be observed. With the increase of NaCl concentration, the polarity of the solution was enhanced. The hydrophobic association of PDA was also promoted, resulting in the formation of larger hydrophobic micro-regions. When the concentration of NaCl increased to 36%, a large-scale, continuous and dense network could be observed. It meant that the molecular chains of PDA had been thoroughly stretched.

From the experimental results of Fig. 3(a)-(c), it was demonstrated that the molecular chain of PDA gradually stretched and released hydrophobic groups with the increase of NaCl concentration in the solutions. The more hydrophobic groups were freely released, the higher the degree of hydrophobic association of PDA. and the larger the hydrophobic micro-regions formed in the solutions. The progressively larger hydrophobic micro-regions led to a decrease in transmittance and an increase in turbidity of the solution. These results further demonstrated that PDA exhibits both anti-polyelectrolyte and hydrophobic association effects. PDA could utilize the anti-polyelectrolyte effect to stretch its molecular chains, thereby releasing benzene rings, sulfonic acid groups, and quaternary ammonium cationic groups. On one hand, this facilitated better adsorption of PDA onto the bentonite surface, forming a thick hydration film that helps maintain the colloidal stability of bentonite. On the other hand, the high-temperature resistance was further enhanced by the hydrophobic association network. PDA

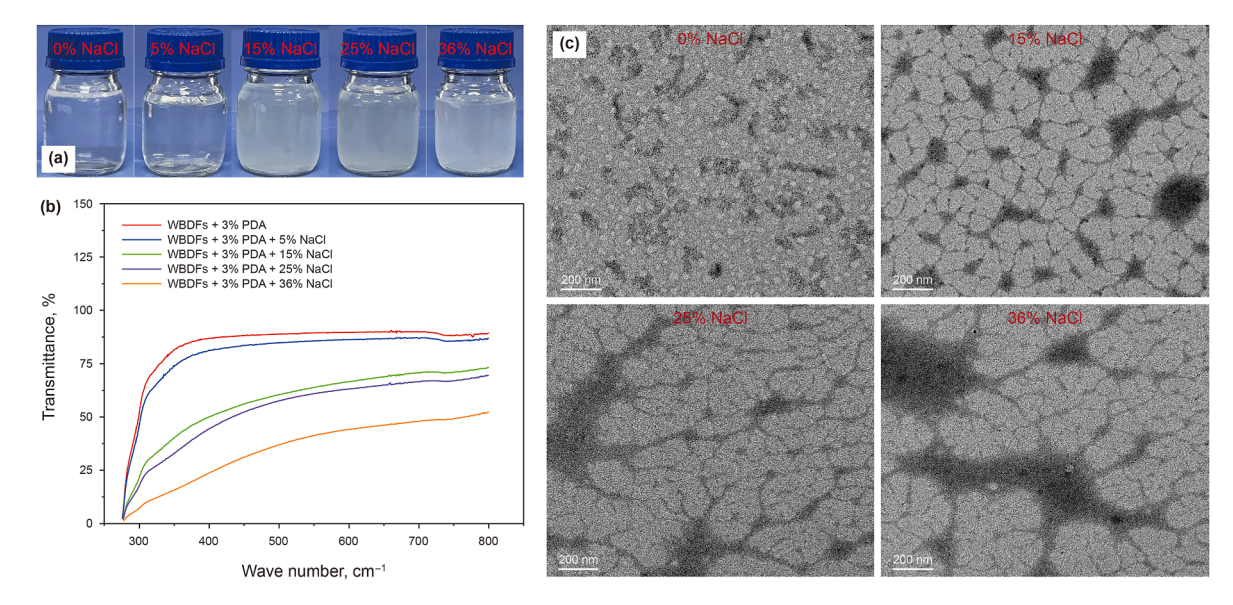


Fig. 3. Characterization of PDA in salt solutions: (a) appearance of PDA salt solutions with different salt concentrations; (b) transmittance of PDA solutions with different salt concentrations; (c) microstructure of PDA with different salt concentrations.

could exhibit excellent salt resistance, even at elevated temperatures.

3.2. Performance evaluation of PDA

3.2.1. Effect of PDA on the performance of WBDFs

PDA-WBDFs were prepared by adding 0%, 0.5%, 1.0%, 1.5%, 2.0%, 2.5%, and 3.0% PDA into water-based drilling fluids (WBDFs). The rheological properties and filtration loss of the PDA-WBDFs were evaluated before and after aging at 220 °C to investigate the effect of PDA on the properties of WBDFs. The results are presented in Fig. 4. It was observed that with increasing PDA concentration, the apparent viscosity (AV), plastic viscosity (PV), and yield point (YP) increased significantly, while the filtration loss was markedly reduced both before and after aging. At a PDA concentration of 3.0%, the AV, PV, and YP reached 93.0 mPa·s, 65.0 mPa·s, and 28.0 Pa, respectively. After aging at 220 °C for 16 h, the AV, PV, and YP were maintained at 39.5 mPa·s, 31.5 mPa·s, and 8.0 Pa, respectively. The API filtration loss (FL_{API}) was reduced to 3.8 mL, representing an 88.10% decrease compared to WBDFs (42.0 mL). The

high-temperature high-pressure filtration loss FL $_{\rm HTHP}$ (180 $^{\circ}$ C, 3.5 $_{\rm MPa)}$ decreased to 30.8 mL, which was 70.94% lower than that of WBDFs (107.0 mL). The results demonstrated that PDA exhibited excellent viscosity-enhancing and filtration loss-reducing capabilities in water-based drilling fluids, even under high-temperature conditions.

3.2.2. Temperature resistance evaluation of PDA in WBDFs

The performance of polymers in drilling fluids typically deteriorates due to the high-temperature hydrolysis of molecular chains, which can lead to poor rheological properties and a significant increase in filtration loss. In order to evaluate the thermal stability of PDA in WBDFs, PDA-WBDFs containing 3.0% PDA were subjected to aging at 180, 200, 220, and 240 °C for 16 h. The rheological properties and filtration loss of PDA-WBDFs were compared with those of WBDFs, and the results are presented in Fig. 5. With increasing temperature from 180 to 240 °C, the AV, PV, and YP of the PDA-WBDFs showed varying degrees of decline. However, all values remained significantly higher than those of the WBDFs. Furthermore, The PDA-WBDFs exhibited markedly lower

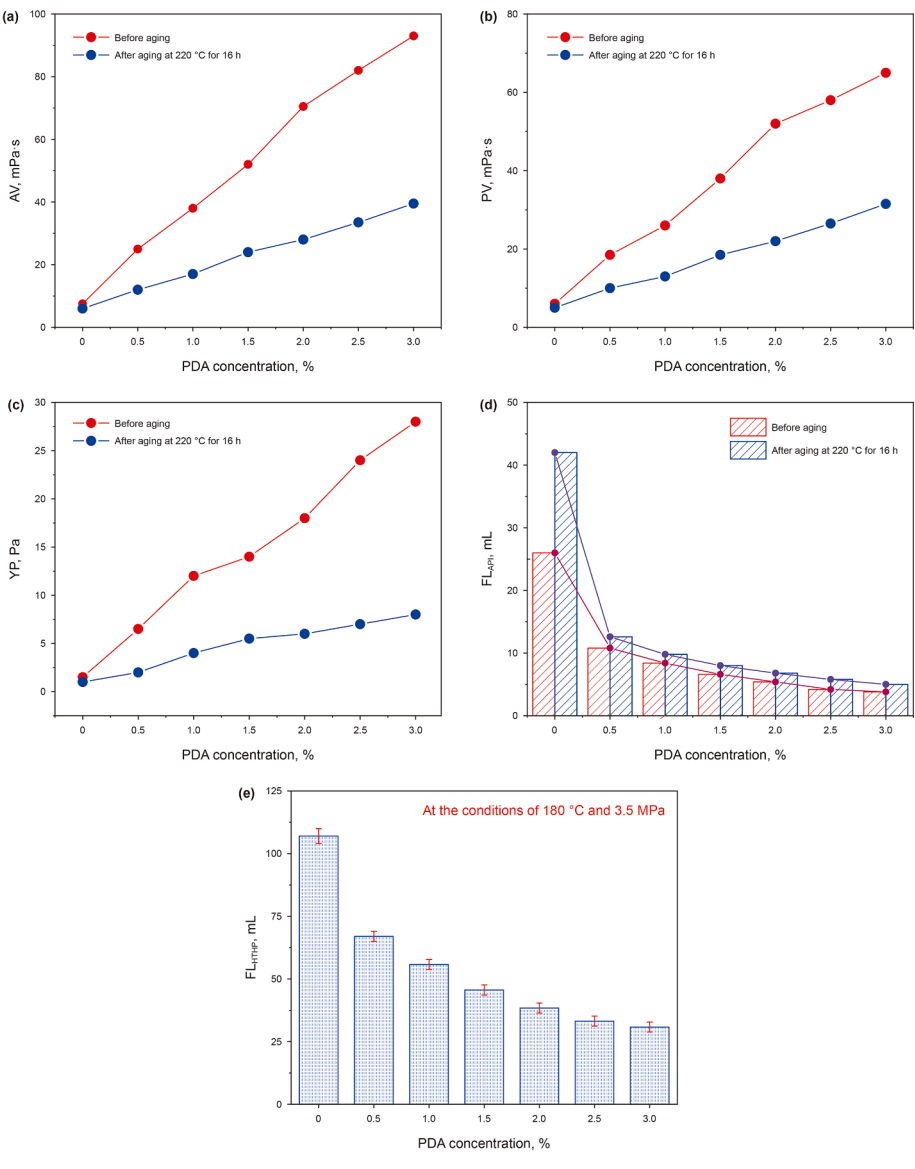


Fig. 4. Effect of PDA on the performance of WBDFs: (a) AV; (b) PV; (c) YP; (d) FL_{API}; (e) FL_{HTHP}.

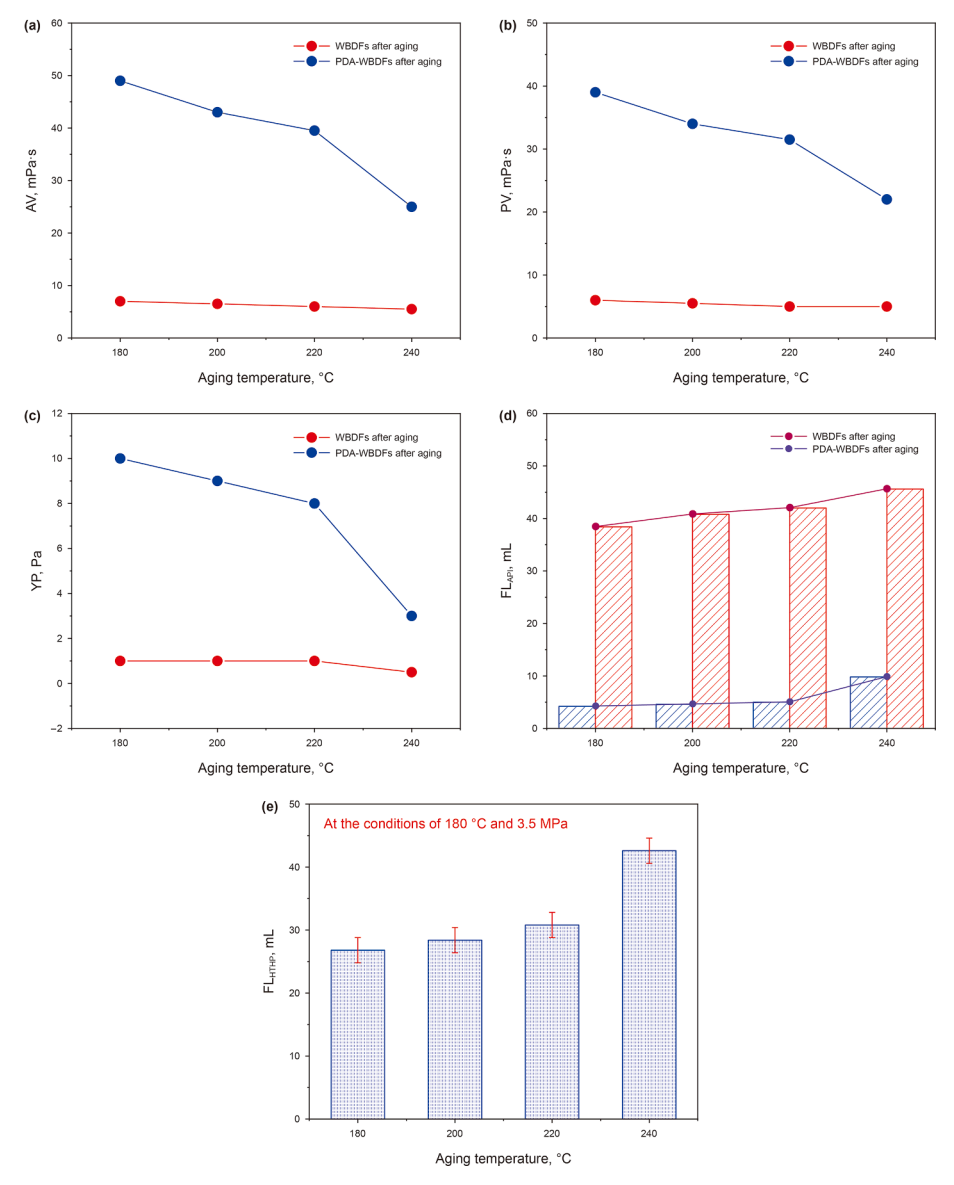


Fig. 5. Temperature resistance evaluation of PDA in WBDFs: (a) AV; (b) PV; (c) YP; (d) FL_{API}; (e) FL_{HTHP}.

filtration loss compared to WBDFs. After aging at 240 °C for 16 h, the FL_{API} was only 9.8 mL, representing a 78.51% reduction compared to the 45.60 mL of WBDFs. The FL_{HTHP (180 °C, 3.5 MPa)} was 37.8 mL, also significantly lower than that of WBDFs. The results demonstrated that PDA effectively maintained the rheological properties and reduced the filtration loss of WBDFs under high-temperature conditions, further confirming its potential as a high-performance additive for extreme drilling environments.

3.2.3. Salt resistance evaluation of PDA

The PDA-SWBDFs were prepared by adding 3% PDA and different amounts of NaCl to WBDFs. The rheological properties and filtration loss of PDA-SWBDFs were evaluated before and after aging at 220 °C to assess the salt resistance of PDA. The results are presented in Fig. 6. As the concentration of NaCl increased from 0% to 36%, the AV, PV, and YP of PDA-SWBDFs gradually decreased before and after aging at 220 °C. This decline could be attributed to the increased adsorption of Na⁺ onto the bentonite surface, which reduced the negative charge of bentonite. Coupled with the thermal degradation of the polymer chains, the network structure

formed between PDA and bentonite was weakened. As a result, the rheological properties diminished with increasing salinity. Nevertheless, the PDA-SWBDFs retained a certain level of viscosity and yield point after aging, owing to the hydrophobic association effect of PDA.

However, the filtration loss of PDA-SWBDFs exhibited an initial increase followed by a subsequent decrease with increasing NaCl concentration. When 5% NaCl was added into drilling fluids, Na⁺ will adsorb on the bentonite surface, reducing the colloidal stability of bentonite and leading to an increase in filtration loss. As shown in Fig. 6(d) and (e), the FL_{API} increased from 5.0 to 7.6 mL and the FL_{HTHP} increased from 30.8 to 45.6 mL. However, as the NaCl concentration increased from 5% to 36%, the FL_{API} decreased from 7.6 to 4.0 mL and the FL_{HTHP} decreased from 45.6 to 32.0 mL. Because the electrostatic force between quaternary ammonium cations and sulfonic acid groups was shielded by a large amount of Na⁺ and the "inner salt bond" was sabotaged. The quaternary ammonium cation groups, sulfonic acid groups and the benzene rings on the polymer chain were released. The release of more quaternary ammonium cation groups was beneficial to maintain

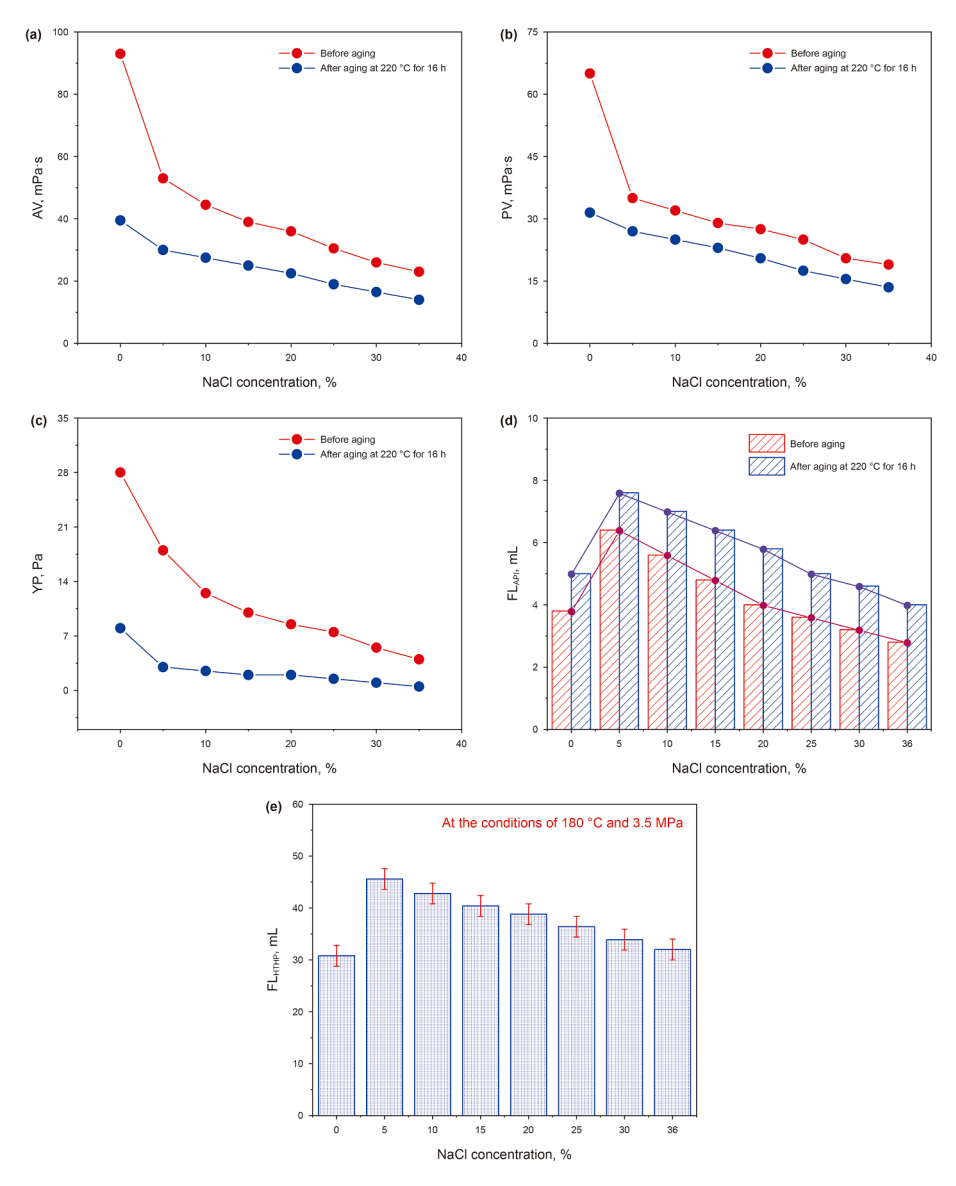


Fig. 6. Salt resistance evaluation of PDA: (a) AV; (b) PV; (c) YP; (d) FLAPI; (e) FLHTHP.

the adsorption capacity of PDA on the bentonite surface, sulfonic acid groups were helpful to increase the hydration film thickness and helped to maintain the colloidal stability of bentonite. Meanwhile, the exposed benzene rings promoted hydrophobic association among PDA chains, contributing to improved thermal stability of PDA. The combined effect of anti-polyelectrolyte and hydrophobic association enabled PDA to effectively reduce the filtration loss under 220 °C and 36% NaCl conditions (Mao et al., 2015). These results confirmed that the temperature resistance of PDA was up to 220 °C in 36% NaCl environment. PDA could partially mitigate the adverse negative effects of high temperature and high salinity to drilling fluids, contributing to maintain the rheological properties and reduce filtration loss.

3.2.4. Temperature resistance evaluation of PDA in SWBDFs

The synergistic effect of high temperature and high salinity will further weaken the adsorption and hydration properties of polymers, leading to the reduction of polymers' performance. The filtrate loss reducers should have abilities of high-temperature and high-salinity resistance at the same time. In order to evaluate the

high-temperature and high-salinity resistance performance of PDA, 3% PDA and 36 wt% NaCl were added into WBDFs to obtain PDA-SWBDFs. The PDA-SWBDFs were aging at 180, 200, 220 and 240 °C respectively for 16 h. The rheological properties and filtration loss of PDA-SWBDFs were measured. The results were showed in Fig. 7. As the aging temperature increased from 180 to 220 °C, the AV, PV and YP of PDA-SWBDFs gradually decreased, but compared with SWDFs, the AV, PV and YP were increased, the filtration loss reduced substantially. When the aging temperature was further increased to 240 °C, the AV, PV and YP of PDA-SWBDFs reduced significantly, they were not much different from those of SWBDFs. Although the FLAPI was only 7.6 mL, FLHTHP (180 °C, 3.5 MPa) reached 63.8 mL, which indicated that the temperature resistance of PDA under 36% NaCl could not reach 240 °C, but could reach 220 °C.

3.2.5. Compared with other filtrate loss reducers

The temperature and salt resistance performances of PDA were compared with other filtrate loss reducers commonly used in oil fields. The filtrate loss reducers (PDA and Driscal D, Dristemp, SP-2

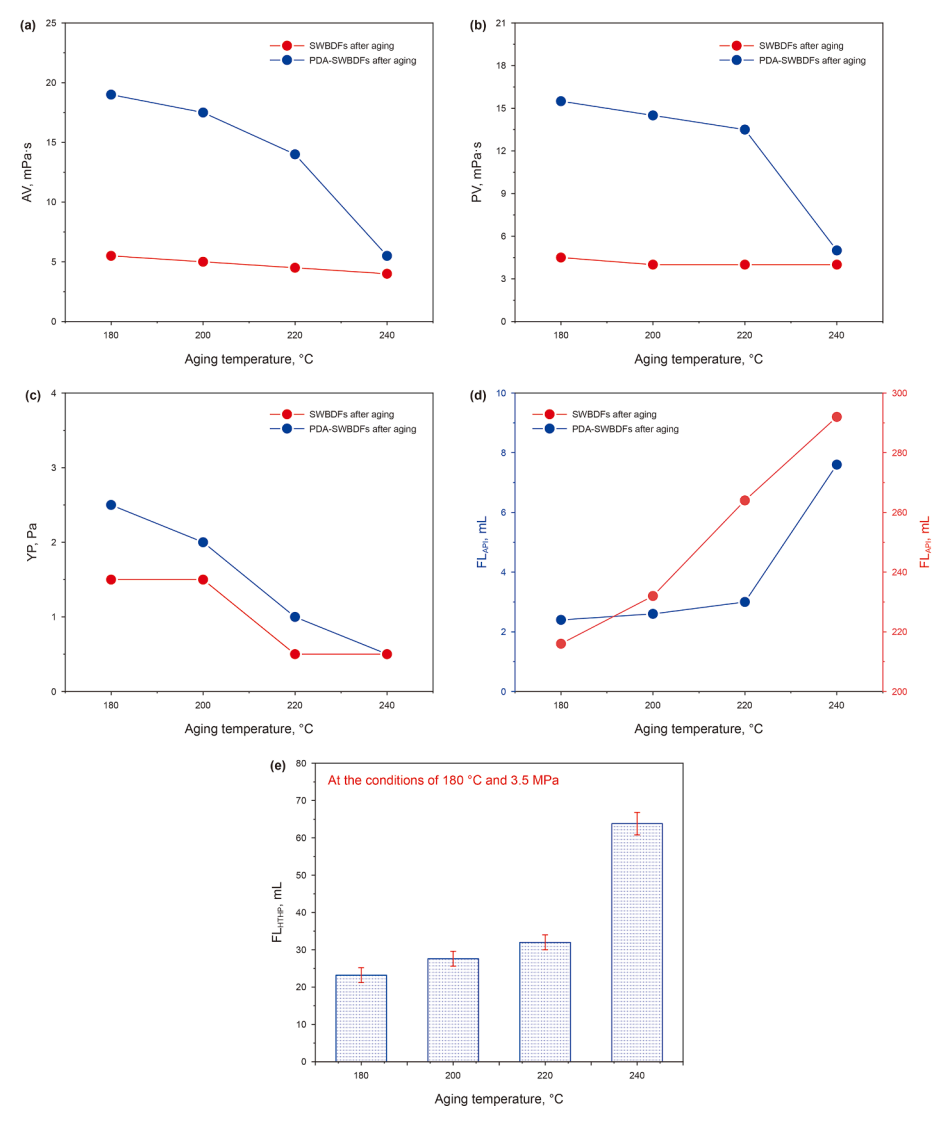


Fig. 7. Temperature resistance evaluation of PDA in SWBDFs: (a) AV; (b) PV; (c) YP; (d) FLAPI; (e) FLHTHP

and SP-1) and 36% NaCl were added to WBDFs to obtain drilling fluids. The concentration of filtrate loss reducers was 3%. The API filtration loss tests of drilling fluids were carried out after aging at 220 °C for 16 h. The results are illustrated in Fig. 8. The FL_{API} of drilling fluids were 24.6, 15.8, 10.4 and 5.4 mL respectively when containing Driscal D, Dristemp, SP-1 and SP-2. And the FL_{API} was only 4.0 mL when containing PDA, which was 83.74%, 74.68%, 61.54% and 25.92% lower than that of Driscal D, Dristemp, SP-2, and SP-1. The results demonstrated that the filtration loss reduction performance of PDA was superior to that of four products under 220 °C and 36% NaCl conditions.

3.3. Mechanism analysis of PDA

3.3.1. Adsorption capacity analysis

The filtrate loss reducers are designed to protect the colloidal stability of bentonite, and they should have excellent adsorption performance. As shown in Fig. 9(a), the adsorption capacity of PDA increased with the increasing of PDA concentration. When 3% of PDA was added into WBDFs, the adsorption capacity of PDA was 328.45 and 248.57 mg/g respectively before and after aging at 220 °C, with a retention rate of 75.68%. Fig. 9(b) represents the

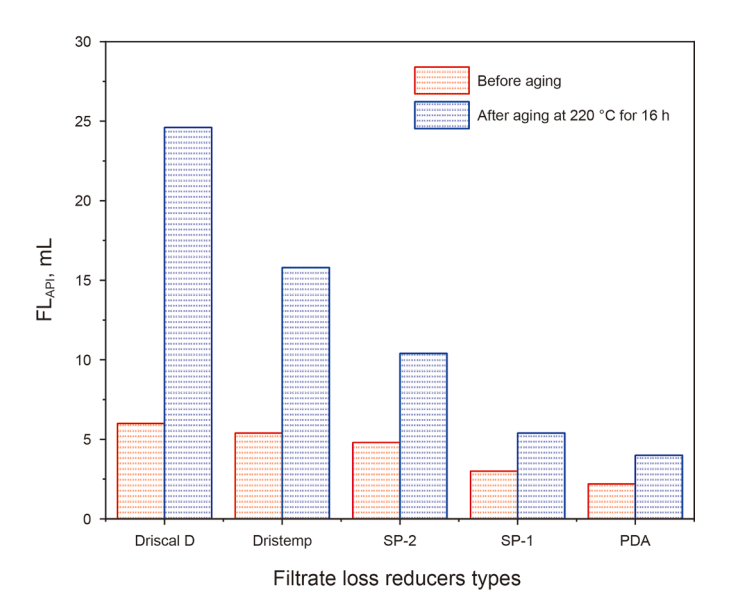


Fig. 8. Comparison of PDA with other filtrate loss reducers.

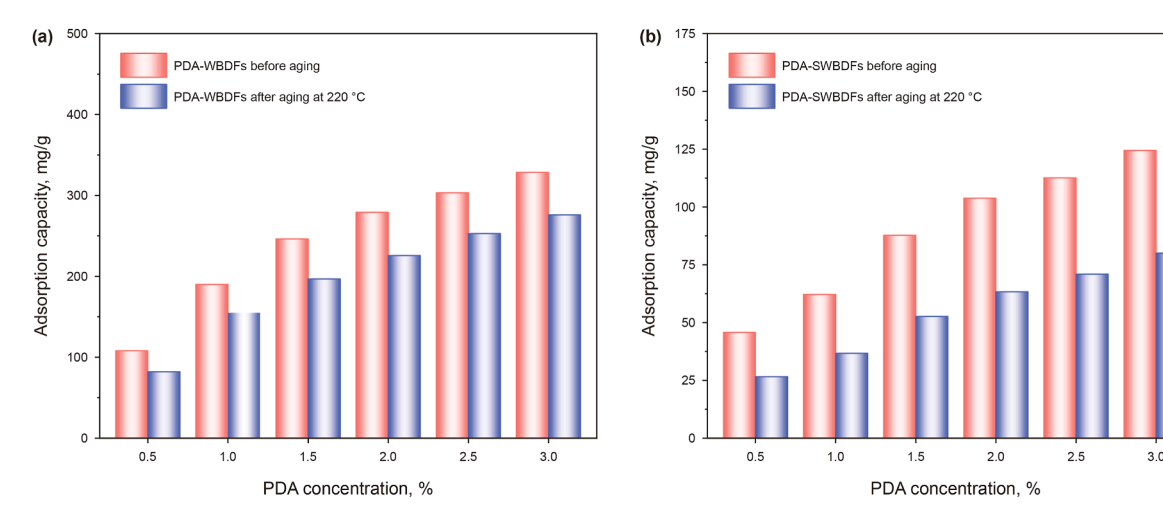


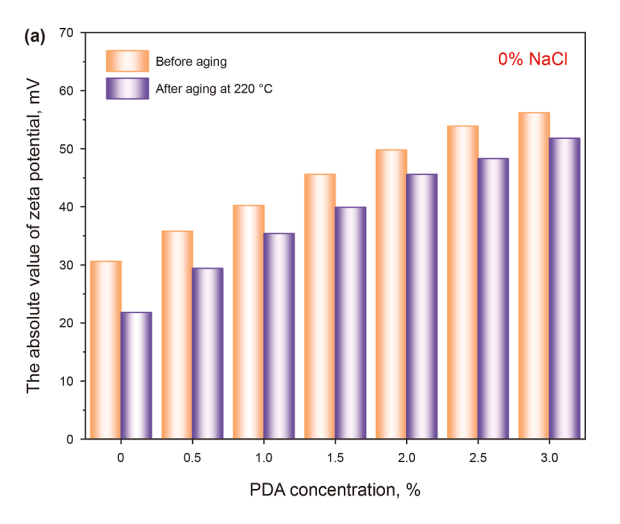
Fig. 9. Adsorption capacity analysis of PDA: (a) adsorption capacity of PDA before and after aging at 220 °C; (b) adsorption capacity of PDA with 36% NaCl before and after aging at 220 °C.

adsorption performance of PDA under 36% NaCl condition. The adsorption capacity of PDA was 124.4 and 79.9 mg/g before and after aging at 220 °C, with a retention rate of 64.23%. The results indicated that PDA had good adsorption stability and remained effectively adsorbed on the bentonite surface under hightemperature and high-salinity conditions. The amide groups and quaternary ammonium cations of PDA could form hydrogen bonds and electrostatic interactions with bentonite surface. Moreover, rigid groups and the hydrophobic association network restricted internal rotation and thermal motion of the polymer chains. The anti-poly electrolyte effect facilitated full extension of molecular chains (Misbah et al., 2023; Liu et al., 2022b; Câmara et al., 2020; Ghazali et al., 2018). The combined effects enabled PDA to adsorb on the bentonite surface strongly, which was conducive to maintaining colloidal stability of bentonite and reducing the filtration loss effectively.

3.3.2. Zeta potential analysis

Drilling fluids are colloidal dispersion systems composed of bentonite as the dispersed phase and water as the continuous phase. After hydration, exchangeable cations dissociate from the bentonite surface, resulting in the formation of a diffuse electric double layer. Consequently, the surface of bentonite always keeps negatively charged. Zeta potential is a crucial parameter for characterizing the colloidal stability of drilling fluids. To intuitively illustrate the changes in zeta potential under high-temperature and high-salinity conditions, the "absolute value of the zeta potential" was adopted in place of the signed value. A higher absolute zeta potential indicates a greater negative charge on the bentonite surface, the greater electrostatic repulsive force between bentonite particles, the better colloidal stability of bentonite. On the contrary, a lower zeta potential reflects a reduction of negative charge on the bentonite surface, the less electrostatic repulsion between bentonite particles, the weaker colloidal stability of bentonite (Wang et al., 2021).

As illustrated in Fig. 10(a), the absolute values of the zeta potential were 30.6 and 21.8 mV of WBDFs before and after aging at 220 °C. The absolute values of the zeta potential were 9.83 and 7.62 mV of WBDFs before and after aging at 220 °C under 36% NaCl condition. This reduction could be attributed to the adsorption of a large quantity of Na⁺ onto the bentonite surface, which compressed the diffused double layer. As a result, the hydration film and electrostatic repulsion of bentonite were weakened, leading to a deterioration of bentonite colloidal stability. As the concentration of PDA increased, the absolute values of zeta potential gradually increased. When the concentration of PDA was 3%, the



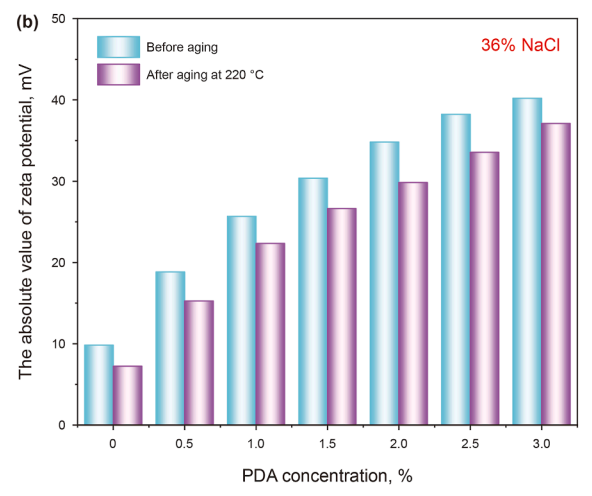


Fig. 10. Zeta potential analysis: (a) zeta potential absolute values of PDA-WBDFs before and after aging at 220 °C; (b) zeta potential absolute values of PDA-SWBDFs before and after aging at 220 °C.

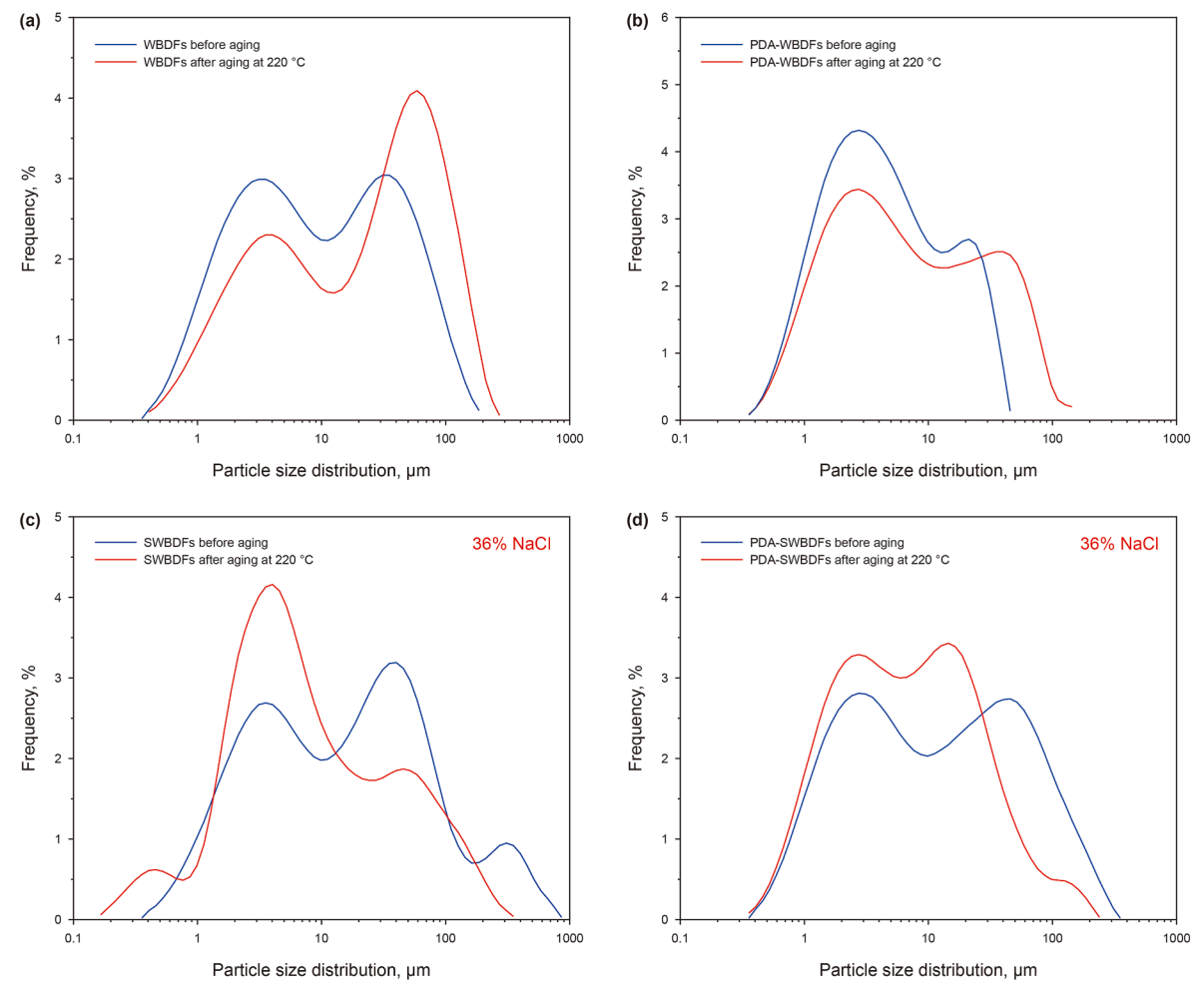


Fig. 11. Particle size distribution analysis of drilling fluids before and after aging at 220 °C: (a) WBDFs; (b) PDA-WBDFs; (c) SWBDFs; (d) PDA-SWBDFs.

absolute values of zeta potential reached 56.2 and 51.8 mV before and after aging at 220 °C. As shown in Fig. 10(b), the absolute values of zeta potential were 40.2 and 37.1 mV before and after aging at 220 °C under 36% NaCl condition. PDA could be effectively adsorbed onto the bentonite surface through amide groups and quaternary ammonium cations. The numerous sulfonic acid groups with strong hydration were able to increase the negative charge and forming a thicker hydration film on bentonite surface. Therefore, PDA improved the colloidal stability of bentonite, promoted the formation of impermeable mud cakes and reduced the filtration loss effectively.

3.3.3. Particle size distribution analysis

As shown in Fig. 11(a), the particle size distribution of the WBDFs shifted to the right after aging at 220 °C. The proportion of bentonite particles in the range of 1–40 μ m decreased, while those in the range of 100–300 μ m increased. Table 2 further confirms that the D_{10} , D_{50} , D_{90} and D_{av} of WBDFs increased significantly after aging at 220 °C, indicating that the colloidal stability of bentonite was undermined and particles agglomeration occurred under high temperature environment. From Fig. 11(b), the particle size distribution shifted to the left When PDA added, which demonstrated that PDA adsorbed on the bentonite surface effectively. PDA increased the thickness of hydration film and enhanced the hydration dispersion property of bentonite. After aging at 220 °C, the D_{10} , D_{50} , D_{90} and D_{av} of PDA-WBDFs were expanded 4.42%, 2.19%,

Table 2 Particle size of drilling fluids before and after aging at 220 $^{\circ}$ C.

Condition	Drilling fluids	D ₁₀ , μm	D ₅₀ , μm	D ₉₀ , μm	D _{av} , μm
Before aging	WBDFs	1.45	8.68	66.97	21.87
	PDA-WBDFs	1.13	5.92	46.65	16.04
	SWBDFs	1.65	16.42	127.01	51.85
	PDA-SWBDFs	1.36	11.24	64.45	30.52
After aging at 220 °C	WBDFs	1.79	24.10	102.52	40.17
	PDA-WBDFs	1.18	6.05	56.91	19.56
	SWBDFs	1.45	5.98	75.94	23.78
	PDA-SWBDFs	1.28	9.77	53.32	26.83

21.99% and 21.94% respectively. The results indicated that PDA could protect the colloidal stability of bentonite and prevent severe agglomeration of bentonite particles under 220 °C. As illustrated in Fig. 11(c), the particle size distribution of SWBDFs shifted to the left after aging at 220 °C, the proportion of bentonite with particle size of 1–20 μm increased, while the proportion of bentonite with particle size of 20–300 μm decreased. Correspondingly, Table 2 shows that the $D_{10},\,D_{50},\,D_{90}$ and D_{av} of bentonite dramatically decreased, indicating that significant dispersion of bentonite occurred in the saturated NaCl environment after aging at 220 °C.

Under high-temperature and high-salinity conditions, the absolute values of zeta potential decreased, the hydration film became thin and the colloidal stability of bentonite was deteriorated. It would lead to a notable reduction in particle size. Probably

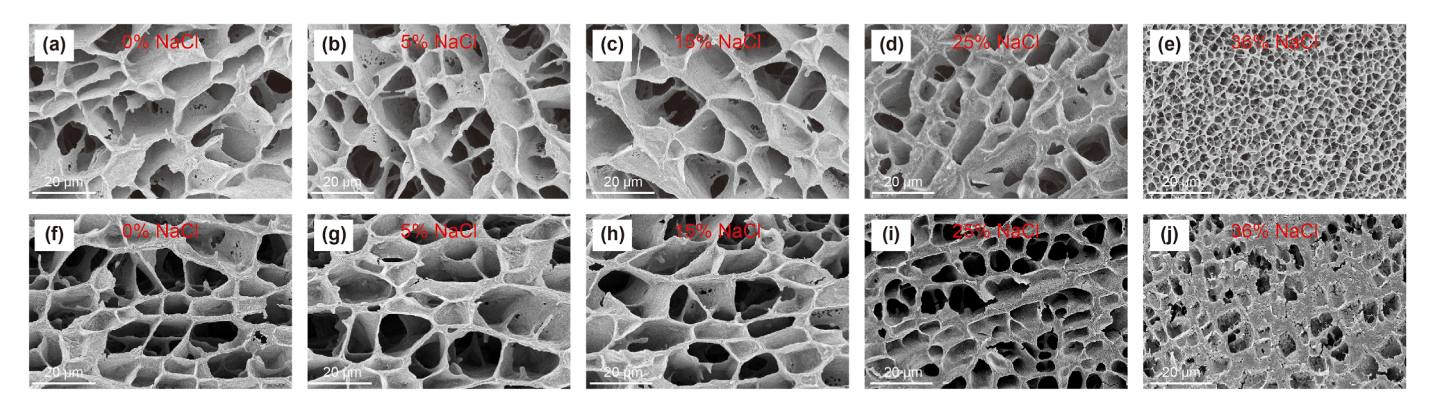


Fig. 12. Spatial network microstructure of PDA-SWBDFs with 0%, 5%, 15%, 25% and 36% NaCl before and after aging at 220 °C: (a)–(e) PDA-SWBDFs before aging; (f)–(g) PDA-SWBDFs after aging at 220 °C.

due to the excessive dispersion of bentonite under hightemperature and high-salinity conditions. The particle size distribution of SWBDFs was not appropriate to form mud cakes with low permeability.

From Fig. 11(d), after adding PDA, it was known that the particle size distribution of PDA-SWBDFs shifted to the left after aging at 220 °C. It also indicated that the bentonite also occurred dispersion. However, the D_{10} , D_{50} , D_{90} and D_{av} were only decreased by 6.25%, 13.08%, 17.27% and 12.09% respectively. The particle size of bentonite did not decrease significantly. PDA could protect the colloidal stability of bentonite effectively, it facilitated the formation of compact mud cakes by preserving an appropriate particle size distribution, and reduced the filtration loss under high-temperature and high-salinity conditions.

3.3.4. Internal microstructure analysis of drilling fluids

The spatial network microstructure of drilling fluids was observed by cryo-scanning electron microscopy in order to further elucidate the mechanism of interaction between PDA and bentonite. As shown in Fig. 12(a)–(e), the internal structure of PDA-SWBDFs exhibited a cross-linked and dense honeycomb-shape network structure. The bentonite could keep the lamellar sheet structure, which maintained a good colloidal dispersion. With the increasing concentration of NaCl, the anti-polyelectrolyte and hydrophobic association of PDA became more pronounced, resulting in a denser network structure in the drilling fluids. As illustrated in Fig. 12(f)–(j), despite the parts of the network of PDA-

SWBDFs were disrupted after aging at 220 °C. The network structure remained cross-linked and compact and the bentonite could retain the filmy sheet structure, indicating that it still maintained the good colloidal stability. The observations demonstrated that possesses excellent temperature and salt resistance. Under high-temperature and high-salinity conditions, PDA adsorbed on the bentonite surface effectively, and formed a stable three-dimensional spatial network with bentonite through antipolyelectrolyte and hydrophobic association. The spatial network structure helped to maintain the stability of the internal structure of drilling fluids. Furthermore, PDA increased the negative charge and the thickness of the hydration film on the bentonite surface, thereby protecting the colloidal stability of bentonite. It was beneficial to facilitate the formation of impermeable mud cakes and reduced the filtration loss.

3.3.5. Microstate analysis of bentonite

The microscopic morphology of bentonite was observed by transmission electron microscopy (TEM) in order to further elucidate the mechanism of PDA. As shown in Fig. 13(a), the bentonite appeared to be the flattened lamellar sheet structure following sufficient hydration, which indicated that the bentonite particles maintained good colloidal dispersion. However, high temperature would cut down the hydration film of bentonite. The colloidal stability was undermined and making it difficult to disperse into the flattened lamellar sheet structure. As illustrated in Fig. 13(b), the bentonite particles became stacked and

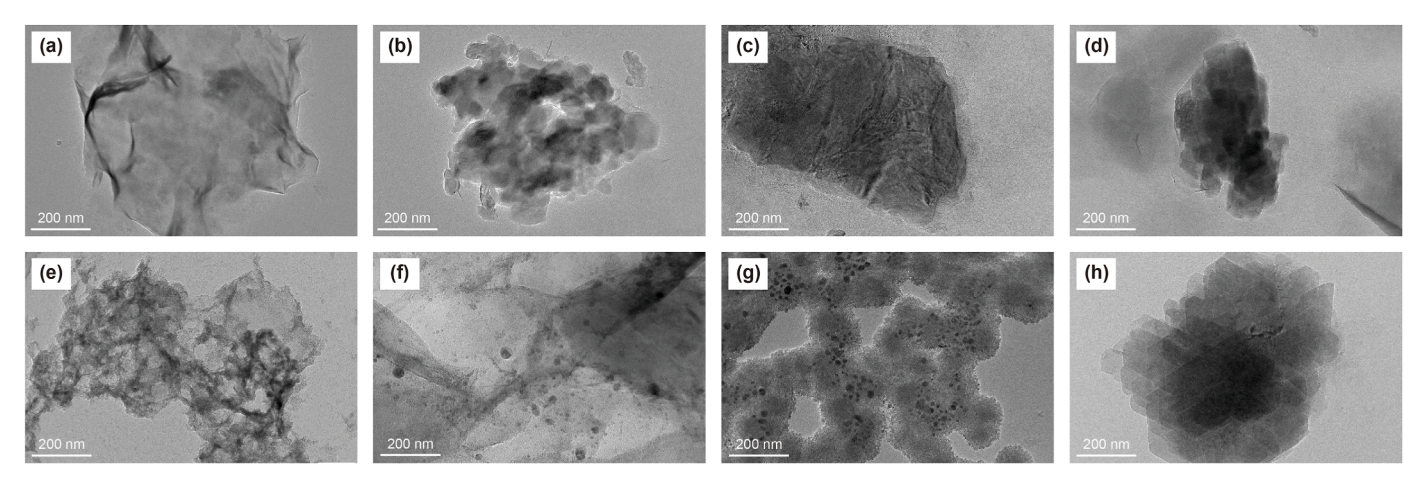


Fig. 13. Microstate of bentonite in drilling fluids before and after aging at 220 °C: (a) WBDFs before aging; (b) WBDFs after aging at 220 °C; (c) SWBDFs before aging; (d) SWBDFs after aging at 220 °C; (e) PDA-SWBDFs before aging; (f) PDA-SWBDFs after aging at 220 °C; (g) Driscal D-SWBDFs before aging; (h) Driscal D-SWBDFs after aging at 220 °C.

transformed into uneven and thicker sheets after aging at 220 °C. After 36% NaCl contamination, the diffuse double layer of bentonite was compressed by Na⁺, the hydration film was further diminished. The hydration and dispersion capacities of bentonite were inhibited. As demonstrated in Fig. 13(c), there were numerous lamellae of bentonite that could be observed and bentonite particles exhibited a notable increase in thickness. As shown in Fig. 13(d), after aging at 220 °C with 36% NaCl, a large number of lamellae of bentonite still remained. The bentonite particles displayed the thicker flake state. The bentonite with thicker flake structure would inevitably lead to the formation of mud cakes with abundant pores and cracks, making it difficult to reduce filtration loss.

In contrast, as shown in Fig. 13(e) and (f), the bentonite was able to maintain the flattened lamellar structure treated with PDA, indicating that the bentonite maintained good colloidal stability under 220 °C and 36% NaCl conditions. However, from Fig. 13(g) and (h), it could be observed that bentonite treated with Driscal D could no longer maintain the flattened lamellar sheet structure, instead appearing as thicker flakes structure in multiple layers. The bentonite with thicker flakes structure was difficult to form the dense and impermeable mud cakes. PDA served as an effective colloidal stabilizer for bentonite under high-temperature and high-salinity conditions. It was helpful to maintain the flattened lamellar structure of bentonite, which was conducive to forming dense and low-permeability mud cakes, thereby effectively reducing filtration loss.

3.3.6. Morphology analysis of mud cakes

As illustrated in Fig. 14(a), there were numerous pores and fractures within the mud cake of WBDFs after aging at 220 °C without PDA. The thickness of the mud cake was 3.35 mm. As shown in Fig. 14(f), after adding 3% PDA to the drilling fluids, the PDA-WBDFs formed a flat, smooth, and dense mud cake without any pores and cracks, the thickness of the mud cake was 0.83 mm. As shown in Fig. 14(b)-(e), after 36% NaCl contamination, the bentonite particles within the mud cake exhibited uneven in size, there were a great deal of pores and grooves between the bentonite particles. The numerous channels facilitated large amount of filtration loss. As shown in Fig. 14(b₁)-(e₁), the mud cakes of SWBDFs were loose and thicker. Because the colloidal stability of bentonite was undermined under high-temperature and high-salinity conditions, the bentonite was unable to maintain the flattened lamellar state. They transformed into thicker flakes. This resulted in the formation of a high permeability mud cake under positive pressure. As illustrated in Fig. 14(g)-(j), after adding 3% PDA, the accumulation of bentonite particles was dense, there were much fewer pores and cracks in mud cakes. As shown in Fig. 14(g_1)–(j_1), all of the mud cakes of PDA-SWBDFs were flat, thin and dense. The thickness of mud cakes was less than 0.9 mm. It was the fact that PDA enabled bentonite particles to maintain the flattened lamellar structure under 220 °C and 36% NaCl. In comparison to the thicker flakes structure, the bentonite of the flattened lamellar structure could be compressed to compact and impermeable mud cakes by positive pressure, reducing the filtration loss eventually.

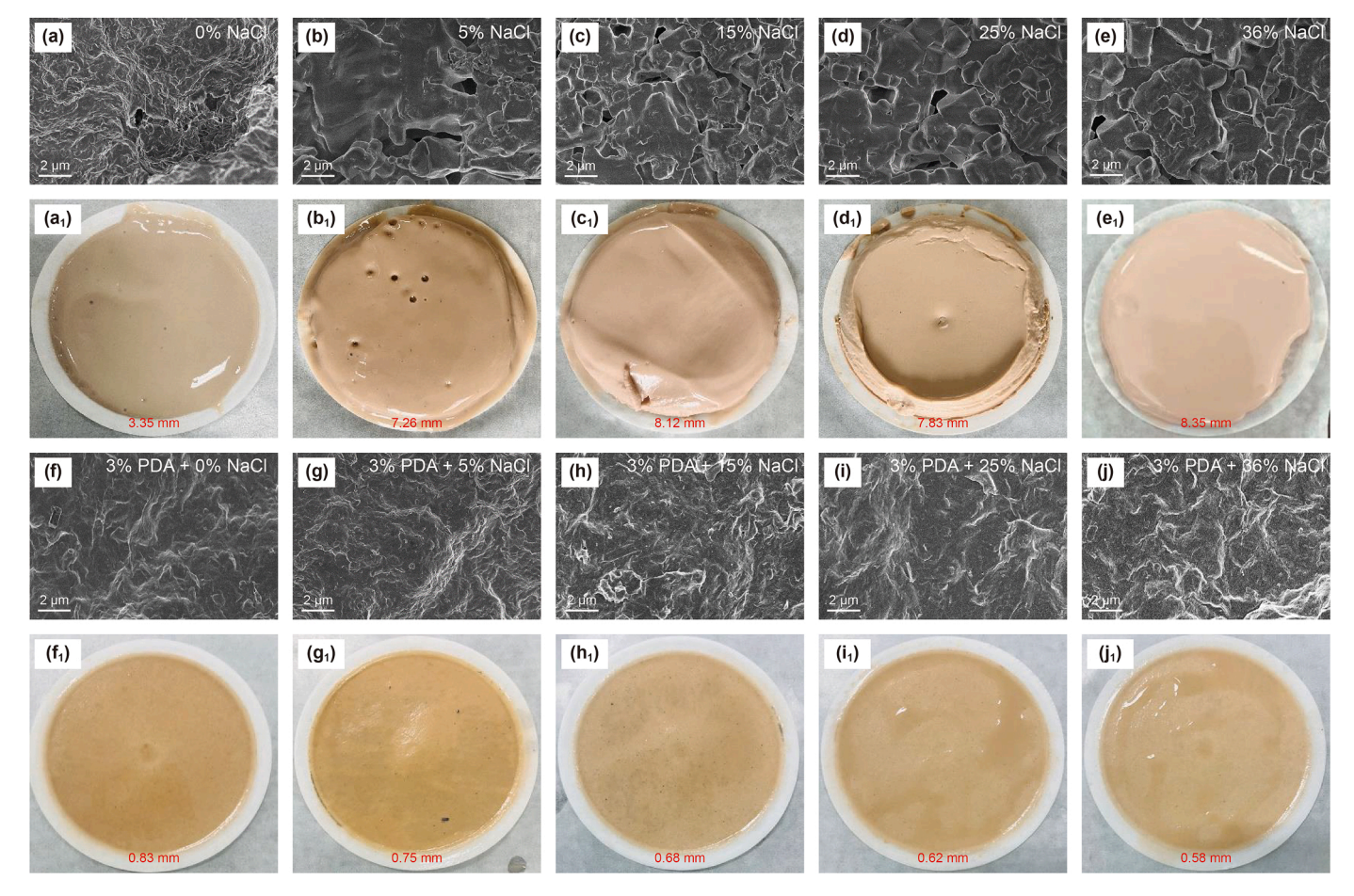


Fig. 14. Morphology analysis of mud cakes of drilling fluids after aging at 220 °C with different concentrations of NaCl: (\mathbf{a})–(\mathbf{e}) micromorphology of mud cakes of SWBDFs; (\mathbf{a}_1)–(\mathbf{e}_1) pictures of mud cakes of SWBDFs; (\mathbf{f})–(\mathbf{j}) micromorphology of mud cakes of PDA-SWBDFs.

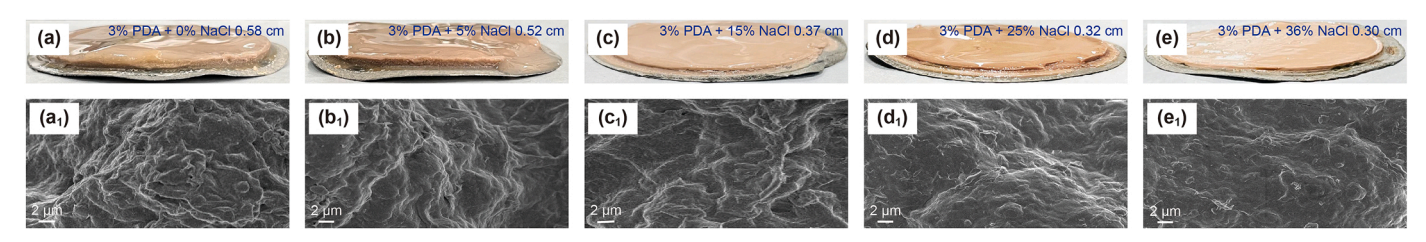


Fig. 15. Morphology analysis of HTHP mud cakes of drilling fluids after aging at 220 °C with different concentrations of NaCl: (a)–(e) pictures of HTHP mud cakes of PDA-SWBDFs; (a₁)–(e₁) micromorphology of HTHP mud cakes of PDA-SWBDFs.

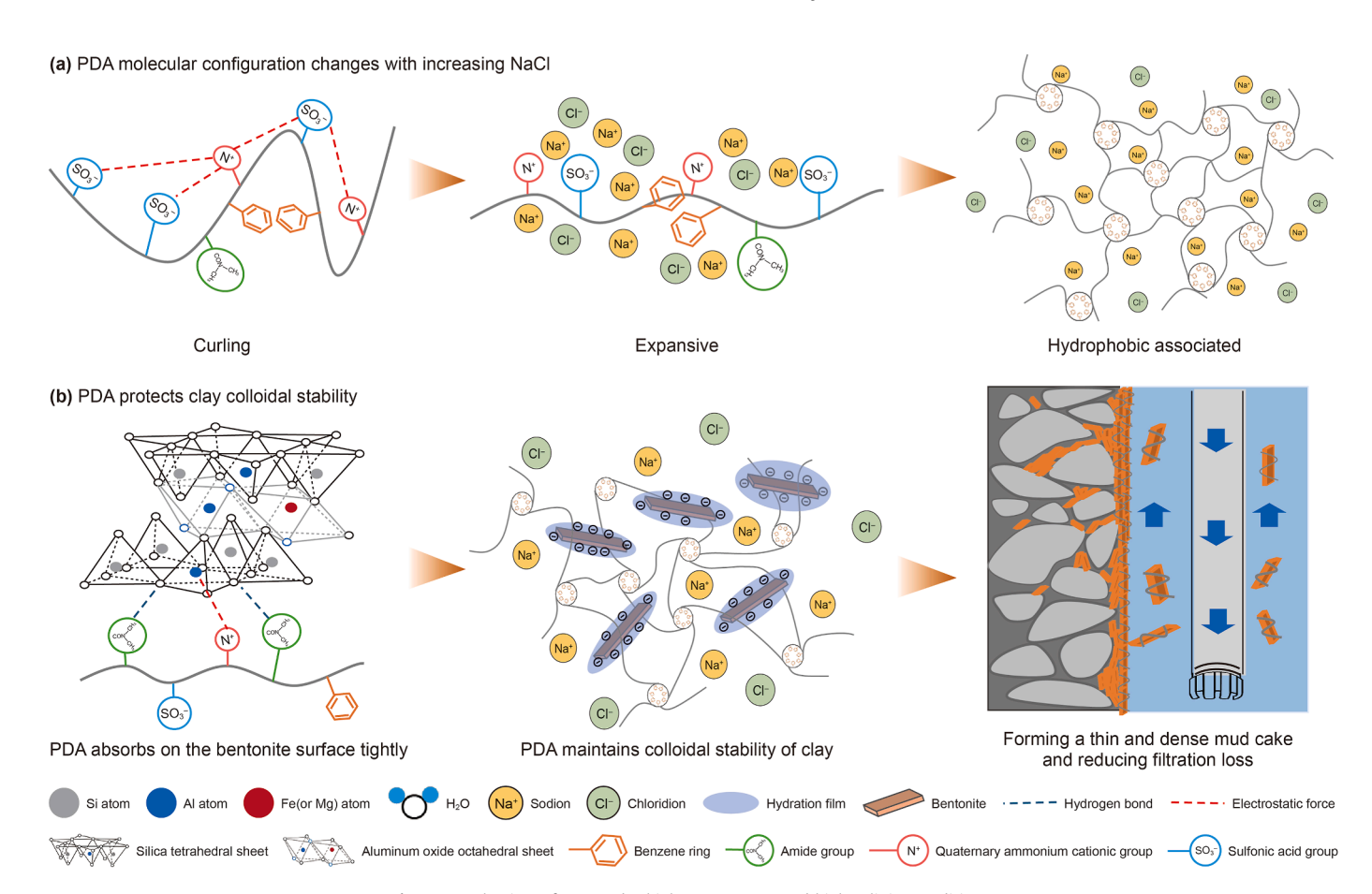
The copolymer PDA will be used in drilling fluids that are exposed to high-temperature, high-pressure and high-salinity environments. Therefore, the HPHT mud cakes can better reflect the effect of filtration loss reduction of drilling fluids. The HTHP mud cakes were fetched out in the HTHP filtration loss tests of Section 3.2.3. From Fig. 15(a) and (b), when the concentration of NaCl was 0% and 5%, the mud cakes were not very thinnish and their surfaces were not particularly flat visually. The thickness was 0.58 and 0.52 cm respectively. From Fig. $15(a_1)$ and (b_1) , there were few pores and cracks between the bentonite particles, although the microscopic surface was not very flat and smooth. As shown in Fig. 15(c)–(e), when the concentration of NaCl increased to 15%, 25% and 36%, the mud cakes became thinner visually, the thickness was 0.37, 0.32 and 0.30 cm correspondently. From Fig. 15(c_1)–(e_1), there were much fewer pores and cracks in the mud cakes, the microscopic surface was flat and dense.

The results illustrated that PDA could effectively improve the quality of mud cakes under the high-temperature, high-pressure

and high-salinity conditions. This was because the bentonite could maintain colloidal stability, the flattened lamellar structure and an appropriate particle size distribution with protection of PDA, then forming a dense and low-porosity mud cakes, thereby reducing the filtration loss.

3.3.7. Mechanism of PDA

The filtration loss reduction mechanism of PDA was revealed by TOC, Cryo-SEM, zeta potential, TEM and SEM. The basic structural unit of bentonite was composed of an aluminium-oxygen octahedral sheet sandwiching two silica-oxygen tetrahedral sheets. Due to lattice substitution, the bentonite particles required to adsorb amount of exchangeable cation (e.g., Na⁺, Ca²⁺) to balance the electrovalence. After hydration, the exchangeable cations dissociated from the bentonite surface to form the diffused double layer. The bentonite surface always carried the negative charge. The exchangeable cations were hydrated, resulting in the formation of a hydration film on the bentonite surface. The electrostatic



 $\textbf{Fig. 16.} \ \ \textbf{Mechanism of PDA under high-temperature and high-salinity conditions}.$

repulsion and hydration film between bentonite particles ensured they could retain good colloidal stability.

However, under high-temperature and high-salinity conditions, the layered structure of bentonite was destroyed, leading to the removal of aluminium-oxygen octahedra and hydroxyl groups. This destruction reduced the negative electricity and weakened the hydration film of bentonite (Aghdam et al., 2020). Furthermore, a large number of electrolyte cations (Na⁺, Ca²⁺) would be adsorbed on the bentonite surface. They compressed the diffused double layer and further diminished the hydration film of bentonite surface. The bentonite would no longer maintain the filmy sheet structure and hardly formed a dense mud cake on the well wall due to the destruction of colloidal stability, which ultimately led to the wellbore instability and caused severe drilling accidents (Yang et al., 2024; Liu et al., 2022c).

PDA contained rigid groups such as benzene ring, quaternary ammonium cationic five-membered ring, sulfonic acid groups, etc., which were resistant to degradation at elevated temperatures (Li et al., 2023e). As shown in Fig. 16, the anti-poly electrolyte and hydrophobic association enabled PDA fully stretch under hightemperature and high-salinity conditions. Meanwhile, PDA was able to adsorb on the bentonite surface strongly through electrostatic force and hydrogen bonding. It was capable of forming a solid and dense honeycomb network structure with bentonite and maintained the stability of the internal structure of drilling fluids. The network structure mitigated the damage of metal cations (Na⁺, Ca²⁺) to the polymer-bentonite network and improved rheological properties of drilling fluids. Moreover, PDA contained a large number of sulfonic acid groups with strong hydration, which could effectively increase the negative electronegativity and the thickness of the hydration film on the bentonite surface. It helped to protect the colloidal stability of bentonite so that the bentonite can preserve the flattened lamellar structure and an appropriate particle size distribution under high-temperature and highsalinity conditions. Consequently, impermeable and dense mud cakes could be formed under positive pressure and reducing the filtration loss eventually.

4. Conclusions

In this study, a hydrophobic association zwitterionic filtrate loss reducer PDA was prepared through emulsion polymerization by using AMPS, DMDAAC, ST, A₁ as raw materials. The results of FTIR, NMR and EA demonstrated that the molecular structure of PDA was consistent with design. The molecular weight of PDA was moderate with a homogeneous distribution. The thermogravimetric analysis demonstrated that the mass retention rate of PDA was 83.0% at 380 °C, PDA was indicative of excellent thermal stability. The UV spectra and TEM analysis of PDA salt solutions indicated that PDA exerted the anti-polyelectrolyte and hydrophobic association effect.

When the concentration of PDA was 3% in WBDFs, the FL_{API} of PDA-WBDF was 9.8 mL and the FL_{HTHP} ($_{180^{\circ}\text{C}}$, $_{3.5\text{ MPa}}$) was 37.8 mL after aging at 240 °C. Under 36% NaCl condition, the FL_{API} of PDA-SWBDF was 4.0 mL and the FL_{HTHP} ($_{180^{\circ}\text{C}}$, $_{3.5\text{ MPa}}$) was 32.0 mL after aging at 220 °C. The performance of PDA was superior to that of the products commonly used in oilfields, such as SP-1, SP-2, Driscal D and Dristemp.

Under high-temperature and high-salinity conditions, PDA could strongly adsorb on the surface of bentonite and formed a dense honeycomb network in drilling fluids. PDA could maintain the colloidal stability of bentonite so that bentonite could kept the flattened lamellar structure and an appropriate particle size distribution, which led to forming dense mud cakes and reducing the filtration loss of drilling fluids effectively.

CRediT authorship contribution statement

Tai-Feng Zhang: Writing – original draft, Methodology, Conceptualization. **Jin-Sheng Sun:** Supervision, Project administration, Funding acquisition. **Jing-Ping Liu:** Writing – review & editing, Project administration, Funding acquisition. **Kai-He Lv:** Project administration, Funding acquisition. **Yuan-Wei Sun:** Methodology, Investigation, Data curation. **Zhe Xu:** Resources, Conceptualization. **Ning Huang:** Resources, Investigation. **Han Yan:** Resources, Investigation.

Data availability

Data will be made available on request.

Declaration of competing interest

The authors declare that they have no known competing financial interests or personal relationships that could have appeared to influence the work reported in this paper.

Acknowledgements

This project is supported by State Key Laboratory of Deep Oil and Gas (No. SKLDOG2024-ZYRC-03). This project is also supported by the Excellent Young Scientists Fund of the National Natural Science Foundation of China (No. 52322401) and the National Natural Science Foundation of China (52288101).

References

- Abdollahi, M., Pourmahdi, M., Nasiri, A.R., 2018. Synthesis and characterization of lignosulfonate/acrylamide graft copolymers and their application in environmentally friendly water-based drilling fluid. J. Petrol. Sci. Eng. 171, 484–494. https://doi.org/10.1016/j.petrol.2018.07.065.
- Aghdam, S.B., Moslemizadeh, A., Kowsari, E., et al., 2020. Synthesis and performance evaluation of a novel polymeric fluid loss controller in water-based drilling fluids: high-temperature and high-salinity conditions. J. Nat. Gas Sci. Eng. 83, 103576. https://doi.org/10.1016/j.jngse.2020.103576.
- Blackman, L., Gunatillake, P., Cass, P., et al., 2019. An introduction to zwitterionic polymer behavior and applications in solution and at surfaces. Chem. Soc. Rev. 48 (3), 757–770. https://doi.org/10.1039/C8CS00508G.
- Câmara, Paulo C.F. da, Madruga, Liszt Y.C., Marques, Nívia do N., et al., 2020. Evaluation of polymer/bentonite synergy on the properties of aqueous drilling fluids for high-temperature and high-pressure oil wells. J. Mol. Liq. 18, 114808. https://doi.org/10.1016/j.molliq.2020.114808.
- Chang, X.F., Sun, J.S., Xu, Z., et al., 2019. A novel nano-lignin-based amphoteric copolymer as fluid-loss reducer in water-based drilling fluids. Colloids Surf. A Physicochem. Eng. Asp. 583, 123979. https://doi.org/10.1016/j.colsurfa.2019.12 3379
- Davoodi, S., Al-Shargabi, M., Wood, D.A., et al., 2023a. Modified-starch applications as fluid-loss reducers in water-based drilling fluids: a review of recent advances. J. Clean. Prod. 434, 140430. https://doi.org/10.1016/j.jclepro.2023.140 430
- Davoodi, S., Al-Shargabi, M., Wood, D.A., et al., 2023b. Thermally stable and salt-resistant synthetic polymers as drilling fluid additives for deployment in harsh sub-surface conditions: a review. J. Mol. Liq. 371, 121117. https://doi.org/10.1016/j.molliq.2022.121117.
- Dickert Jr., J.J., Heilweil, I.J., 1986. Vinyl sulfonate amide copolymer and terpolymer combinations for control of filtration in water-based drilling fluids at high temperature. U.S. Patent 4,608,182.
- Gao, S.D., Lin, D., Li, A., et al., 2024. Synergistic effects of covalent crosslinking and hydrophobic association on enhancing thermal and salt resistance of polymeric filtrate reducer. J. Mol. Liq. 407, 125204. https://doi.org/10.1016/j. molliq.2024.125204.
- Gautam, Ś., Guria, C., 2020. Optimal synthesis, characterization, and performance evaluation of high-pressure high-temperature polymer-based drilling fluid: the effect of viscoelasticity on cutting transport, filtration loss, and lubricity. SPE J. 25 (3), 1333–1350. https://doi.org/10.2118/200487-PA.
- Gautam, S., Guria, C., Rajak, V.K., 2022. A state of the art review on the performance of high-pressure and high-temperature drilling fluids: towards understanding the structure-property relationship of drilling fluid additives. J. Petrol. Sci. Eng. 213, 110318. https://doi.org/10.1016/j.petrol.2022.110318.
- Ghazali, N.A., Naganawa, S., Masuda, Y., 2018. Development of modified Rhizophora spp. Tannin biopolymer additive in drilling fluid system for high

- temperature well applications. In: IADC/SPE Asia Pacific Drilling Technology Conference and Exhibition, Bangkok, Thailand. https://doi.org/10.2118/191080-MS
- Huang, X.B., Sun, J.S., Lv, K.H., et al., 2023. A high-temperature resistant and high-density polymeric saturated brine-based drilling fluid. Petrol. Explor. Dev. 50 (5), 1215–1224. https://doi.org/10.1016/S1876-3804(23)60460-4.
- Huang, X.B., Dai, Z.W., Zhang, C., et al., 2024. Improving the performance of a polyamine shale inhibitor by introducing a hydrophobic group in oil and gas development. Fuel (Guildf.) 355, 129435. https://doi.org/10.1016/j.fuel.2023.12
- Jhan, Y., Tsay, R., 2014. Salt effects on the hydration behavior of zwitterionic poly (sulfobetaine methacrylate) aqueous solutions. J. Taiwan Inst. Chem. Eng. 45 (6), 3139–3145. https://doi.org/10.1016/j.jtice.2014.08.022.
- Jiang, G.C., Ni, X.X., Li, W.Q., et al., 2020. Super-amphiphobic, strong self-cleaning and high-efficiency water-based drilling fluids. Pet. Explor. Dev. 47 (2), 421–429. https://doi.org/10.1016/S1876-3804(20)60059-3.
- Katende, A., Boyou, N. V., Ismail, I., et al., 2019. Improving the performance of oil based mud and water based mud in a high temperature hole using nanosilica nanoparticles. Colloids Surf. A Physicochem. Eng. Asp. 577, 645–673. https:// doi.org/10.1016/j.colsurfa.2019.05.088.
- Kumar, R., Fredrickson, G.H., 2009. Theory of polyzwitterion conformations. JCP 131 (10), 104901. https://doi.org/10.1063/1.3216107.
 Li, J., Sun, J.S., Lv, K.H., et al., 2022. Temperature-and salt-resistant micro-cross-
- Li, J., Sun, J.S., Lv, K.H., et al., 2022. Temperature-and salt-resistant micro-cross-linked polyampholyte gel as fluid-loss additive for water-based drilling fluids. Gels 8 (5), 289. https://doi.org/10.3390/gels8050289.
- Li, M.C., Liu, X.Y., Lv, K.H., et al., 2023a. Cellulose nanomaterials in oil and gas industry: current status and future perspectives. Prog. Mater. Sci. 139, 101187. https://doi.org/10.1016/j.pmatsci.2023.101187.
- Li, H., Sun, J.S., Xie, S.X., et al., 2023b. Controlling filtration loss of water-based drilling fluids by anionic copolymers with cyclic side groups: high temperature and salt contamination conditions. Colloids Surf. A Physicochem. Eng. Asp. 676, 132089. https://doi.org/10.1016/j.petrol.2021.109808.
- Li, H., Huang, X.B., Sun, J.S., et al., 2023c. Multi-ring side groups copolymer as an effective filtration control additive for water-based drilling fluids under high temperature and salt contamination. Geoenergy Sci. Eng. 225, 211690. https://doi.org/10.1016/j.geoen.2023.211690.
- Li, H., Huang, X.B., Sun, J.S., et al., 2023d. Application of zwitterionic copolymer as a filtration control agent against high temperature and high salinity for waterbased drilling fluids. J. Mol. Liq. 385, 122419. https://doi.org/10.1016/j. mollig.2023.122419.
- Li, J., Sun, J.S., Lv, K.H., et al., 2023e. A zwitterionic copolymer as fluid loss reducer for water-based drilling fluids in high temperature and high salinity conditions. Geoenergy Sci. Eng. 222, 111200. https://doi.org/10.1016/j.petrol.2022.11 1200.
- Li, J., Ji, Y.X., Ni, X.X., et al., 2024. A micro-crosslinked amphoteric hydrophobic association copolymer as high temperature-and salt-resistance fluid loss reducer for water-based drilling fluids. Pet. Sci. 21 (3), 1980–1991. https://doi.org/10.1016/j.petsci.2024.01.021.
- Liu, X.L., Yuan, Z.Y., Wang, A., et al., 2020. Cellulose nanofibril-polymer hybrids for protecting drilling fluid at high salinity and high temperature. Carbohydr. Polym. 229, 115465. https://doi.org/10.1016/j.carbpol.2019.115465.
- Liu, L.M., Sun, J.S., Wang, R., et al., 2022a. Synthesis of a new high temperature and salt resistant zwitterionic filtrate reducer and its application in water-based drilling fluid. Colloids Surf. A Physicochem. Eng. Asp. 651, 129730. https:// doi.org/10.1016/j.colsurfa.2022.129730.
- Liu, L.M., Sun, J.S., Wang, R., et al., 2022b. New zwitterionic polymer as a highly effective salt-and calcium-resistant fluid loss reducer in water-based drilling fluids. Gels 8 (11), 735. https://doi.org/10.3390/gels8110735.
- Liu, J.P., Zhang, T.F., Sun, Y.W., et al., 2022c. Insights into the high temperature-induced failure mechanism of bentonite in drilling fluid. Chem. Eng. J. 445, 136680. https://doi.org/10.1016/j.cej.2022.136680.
- Liu, Y.L., Djouonkep, L.D.W., Yu, B.Y., et al., 2024. Preparation of ultra-high temperature resistant cyclodextrin-based filtration loss reducer for water-based drilling fluids. Molecules 29 (12), 2933. https://doi.org/10.3390/molecules2912 2933.
- Lu, J., Chen, H.B., Luo, X., et al., 2024. A simple photocatalytic assisted strategy by MIL-100 (Fe) for fabrication of polymer based on H-bonding as filtrate reducer to resist salt and temperature in ultra-deep wells. Fuel (Guildf.) 359, 130377. https://doi.org/10.1016/j.fuel.2023.130377.
- Lucas, J.M., Enright, D.P., Perricone, A.C., 1981. Drilling fluid containing a copolymer filtration control agent. U.S. Patent, 4,293,427.
- Luo, Y.X., Lin, L., Luo, P.Y., et al., 2023. Polymer nanocomposite ADA@ SM as a high-temperature filtrate reducer for water-based drilling fluids and its filtration loss mechanism. Colloids Surf. A Physicochem. Eng. Asp. 672, 131701. https://doi.org/10.1016/j.colsurfa.2023.131701.
- Ma, X.P., Yang, M., Zhang, M., 2020. Synthesis and properties of a betaine type copolymer filtrate reducer. Chem. Eng. Process 153, 107953. https://doi.org/ 10.1016/j.cep.2020.107953.

- Mao, H., Qiu, Z.S., Shen, Z.H., et al., 2015. Hydrophobic associated polymer based silica nanoparticles composite with core-shell structure as a filtrate reducer for drilling fluid at utra-high temperature. J. Petrol. Sci. Eng. 129, 1–14. https://doi.org/10.1016/j.petrol.2015.03.003.
- Misbah, B., Sedaghat, A., Balhasan, S., et al., 2023. Enhancing thermal stability and filtration control for water-based drilling fluid using viscosifier polymers and potassium chloride additives. Geoenergy Sci. Eng. 230, 212235. https://doi.org/10.1016/j.geoen..212235.
- Mu, L.X., Ji, Z.F., 2019. Technological progress and development directions of PetroChina overseas oil and gas exploration. Petrol. Explor. Dev. 46 (6), 1088–1099. https://doi.org/10.1016/S1876-3804(19)60265-X.
- Muthukumar, M., 2017. 50th anniversary perspective: a perspective on polyelectrolyte solutions. Macromolecules 50 (24), 9528–9560. https://doi.org/10.1021/acs.macromol.7b01929.
- Oriji, A.B., Dosunmu, A., 2012. Design and application of drilling fluids for HPHT Well-A case study of Mafia Field. SPE J. 44 (23), 9703–9711. https://doi.org/10.2118/151642-MS.
- Sepehri, S., Soleyman, R., Varamesh, A., et al., 2018. Effect of synthetic water-soluble polymers on the properties of the heavy water-based drilling fluid at high pressure-high temperature (HPHT) conditions. J. Petrol. Sci. Eng. 166, 850–856. https://doi.org/10.1016/j.petrol.2018.03.055.
- Son, A., Ballard, T., Loftin, R., 1987. Temperature-stable polymeric fluid-loss reducer tolerant to high electrolyte contamination. SPE Drill. Complet. 2 (3), 209–217. https://doi.org/10.2118/13160-PA.
- Sun, J.S., Chang, X.F., Lv, K.H., et al., 2020. Salt-responsive zwitterionic copolymer as tackifier in brine drilling fluids. J. Mol. Liq. 319, 114345. https://doi.org/10.1016/j.molliq.2020.114345.
- Sun, J.S., Zhang, X.F., Lv, K.H., et al., 2022a. Synthesis of hydrophobic associative polymers to improve the rheological and filtration performance of drilling fluids under high temperature and high salinity conditions. J. Petrol. Sci. Eng. 209, 109808. https://doi.org/10.1016/j.petrol.2021.109808.
- Sun, J.S., Wang, Z.L., Liu, J.P., et al., 2022b. Notoginsenoside as an environmentally friendly shale inhibitor in water-based drilling fluid. Petro Sci 19 (2), 608–618. https://doi.org/10.1016/j.petsci.2021.11.017.
- Sun, J.S., Yang, J.B., Bai, Y.R., et al., 2024. Research progress and development of deep and ultra-deep drilling fluid technology. Petrol. Explor. Dev. 51 (4), 1022–1034. https://doi.org/10.1016/S1876-3804(24)60522-7.
- Tang, Z.C., Qiu, Z.S., Zhong, H.Y., et al., 2022. Novel acrylamide/2-acrylamide-2-3methylpropanesulfonic acid/styrene/maleic anhydride polymer-based CaCO₃ nanoparticles to improve the filtration of water-based drilling fluids at high temperature. Gels 8 (5), 322. https://doi.org/10.3390/gels8050322.
- Tehrani, A., Gerrard, D., Young, S., et al., 2009. Environmentally Friendly Water-Based Fluid for HPHT Drilling. In: SPE International Conference on Oilfield Chemistry, The Woodlands, Texas, USA. https://doi.org/10.2118/121783-MS.
- Tonge, S.R., Tighe, B.J., 2001. Responsive hydrophobically associating polymers: a review of structure and properties. Adv. Drug Deliv. Rev. 53 (1), 109–122. https://doi.org/10.1016/S0169-409X(01)00223-X.
- Wang, G.S., Jiang, G.C., Yang, J., et al., 2021. Novel N, N-dimethylacrylamide copolymer containing multiple rigid comonomers as a filtrate reducer in water-based drilling fluids and mechanism study. J. Appl. Polym. 138 (39), 51001. https://doi.org/10.1002/app.51001.
- Wu, Y.M., Zhang, B.Q., Wu, T., et al., 2001. Properties of the forpolymer of N-vinylpyrrolidone with itaconic acid, acrylamide and 2-acrylamido-2-methyl-1-propane sulfonic acid as a fluid-loss reducer for drilling fluid at high temperatures. Colloid Polym. Sci. 279, 836–842. https://doi.org/10.1007/s003960100494.
- Yang, J., Wang, R., Sun, J.S., et al., 2024. Comb polymer/layered double hydroxide (LDH) composite as an ultrahigh temperature filtration reducer for waterbased drilling fluids. Appl. Surf. Sci. 645, 158884. https://doi.org/10.1016/j. apsusc.2023.158884.
- Yao, G.S., Wu, X.Z., Sun, Z.D., et al., 2018. Status and prospects of exploration and exploitation key technologies of the deep petroleum resources in onshore China. Nat. Gas Geosci. 3 (1), 25–35. https://doi.org/10.1016/j.jnggs.2018. 03.002.
- Zhang, Y., Mao, J.C., Zhao, J.Z., et al., 2019. Preparation of a hydrophobic-associating polymer with ultra-high salt resistance using synergistic effect. Polymers 11 (4), 626. https://doi.org/10.3390/polym11040626.
- Zhao, Z.G., Pu, X.L., Xiao, L., et al., 2015. Synthesis and properties of high temperature resistant and salt tolerant filtrate reducer N, N-dimethylacrylamide 2acrylamido-2-methyl-1-propyl dimethyl diallyl ammonium chloride N-vinylpyrrolidone quadripolymer. J. Polym. 35 (7), 627–635. https://doi.org/10.1515/ polyeng-2014-0260.
- Zhong, H.Y., Li, S.S., Liu, W.L., et al., 2023. Nano-CaCO₃/AA-AM-AMPS cross-linked polymer core-shell structural nanocomposite as high temperature and high salt resistant filtration reducer in water-based drilling fluid. Geoenergy Sci. Eng. 224, 211590. https://doi.org/10.1016/j.geoen.2023.211590.